Title: A novel subset of follicular helper-like MAIT cells has capacity for B cell help and antibody production in the mucosa.

Author List: Owen Jensen[1,2], Shubhanshi Trivedi[1], Jeremy D. Meier[3, 4], Keke Fairfax[2], J. Scott Hale[2], Daniel T. Leung[1, 2*]

[1] Division of Infectious Diseases, Department of Internal Medicine, University of Utah School of Medicine, Salt Lake City, USA
[2] Division of Microbiology & Immunology, Department of Pathology, University of Utah School of Medicine, Salt Lake City, USA
[3] Division of Otolaryngology-Head and Neck Surgery, University of Utah School of Medicine, Salt Lake City, USA
[4] Primary Children's Hospital, Salt Lake City, USA

* Corresponding author: daniel.leung@utah.edu

One Sentence Summary: We identified and characterized a novel subset of T follicular helper-like MAIT (MAITfh) cells that has the capacity to provide B cell help, and show the sufficiency of MAIT cells to promote production of pathogen-specific IgA antibodies and B cell differentiation in mucosal challenge.

Abstract

Mucosal-associated invariant T (MAIT) cells are innate-like T lymphocytes that aid in protection against bacterial pathogens at mucosal surfaces via release of inflammatory cytokines and cytotoxic molecules. Recent evidence suggests MAIT cells are capable of providing B cell help. In this study, we describe a previously unreported population of $CXCR5^+$ T follicular helper (Tfh)-like MAIT cells, MAITfh, that have the capacity to provide B cell help within mucosal lymphoid organs. MAITfh cells are preferentially located near germinal centers in human tonsils and express the classical Tfh-associated transcription factor, B-cell lymphoma 6 (BCL-6), co-stimulatory markers, inducible T cell costimulatory (ICOS) and programmed death receptor 1 (PD-1), and cytokines, interleukin (IL)-21. Furthermore, we demonstrate the ability of MAIT cells to provide B cell help *in vivo* following mucosal challenge with *Vibrio cholerae*. Specifically, we show that adoptive transfer of MAIT cells into αβ T cell-deficient mice promoted B cell differentiation and increased serum *V. cholerae*-specific IgA responses. Our data demonstrate the capacity of MAIT cells to participate in adaptive immune responses, and suggest that MAIT cells may be potential targets for mucosal vaccines.

37 **Introduction**

38 Mucosal surfaces are in constant contact with both commensal and pathogenic microbes. One of the
39 primary means of protection against invading pathogens is the production of secretory IgA and IgM by
40 plasmablasts (PB) and plasma cells (PC) (*1*). In the lamina propria of the gut and lung, T independent low
41 affinity IgA is produced against non-protein antigens by short-lived PBs. Conversely, T dependent high
42 affinity antibodies against protein antigens are typically generated during germinal center reactions
43 between T follicular helper (Tfh) and follicular B cells within local lymph nodes (LNs) or mucosal
44 associated lymphoid tissues (MALT) (*2*). T follicular helper (Tfh) cells migrate to B cell follicles via
45 upregulation of CXCR5 and downregulation of CCR7 (*3*). Within GCs, Tfh cells highly express the
46 lineage-defining transcription factor, BCL6, and co-stimulatory molecules, PD1, ICOS, and CD40L (*4*).
47 PD1 is important for Tfh GC positioning and function (*5*), while ICOS (*6*) and CD40L (*7*) engagement
48 with B cells are essential for Tfh activation and GC formation (*4*). Tfh also produce cytokines, such as IL-
49 21, that promote GC B cell responses (*8*).

50

51 Although Tfh cells are the primary drivers of T dependent GC responses, innate T cells, including
52 invariant Natural Killer T (iNKT) cells and γδ T cells, also have Tfh like subsets capable of B cell help. In
53 particular, iNKT cells have been well established in mice to provide both cognate and non-cognate help to
54 B cells (*9–18*). Murine iNKTfh cells engage in cognate help leading to germinal center formation, and
55 antibody class switching and production (*12*, *14*, *18*). iNKTfh cells have also been shown to promote non-
56 cognate B cell help by licensing dendritic cells to recruit and activate Tfh cells (*10*, *11*). $CXCR5^{+}$ γδ T
57 cells can promote antibody production *in vitro* (*19*, *20*), and promote Tfh differentiation *in vivo* (*21*).
58 More recent evidence suggests that another type of innate-like lymphocyte, Mucosal-associated invariant
59 T (MAIT) cells, are capable of B cell help (*22–26*).

60

61 MAIT cells are innate-like αβ T cells defined by the expression of an invariant α chain, generally Vα7.2
62 linked to Jα33, 12 or 20 in humans and Vα19 linked to Jα33 in mice, and a limited array of TCRβ chains
63 (*27–29*). MAIT cells are highly enriched in human blood, liver and mucosa and are appreciated for their
64 rapid ability to respond to microbial Vitamin B metabolites presented on the MHC class I related protein,
65 MR1, or cytokine stimulation (*30–33*). Upon stimulation, MAIT cells produce pro-inflammatory
66 cytokines including IFNγ, TNFα, and IL-17A and cytotoxic molecules including Granzyme B and
67 Perforin (*34–36*). Furthermore, using MAIT deficient mice ($MR1^{-/-}$), several studies have exemplified the
68 importance of MAIT cells in immunity against mucosal bacterial pathogens (*37–40*).
69
70 Recent evidence suggests MAIT cells play a role in adaptive immune responses through B cell help.
71 Analysis of human peripheral blood MAIT cells and serum antibody responses following *Vibrio cholerae*
72 infection (*22*) and *Shigella* vaccination (*35*), revealed strong associations between MAIT frequency and
73 activation with polysaccharide-specific IgA and IgG responses, but not with protein antibody responses
74 (*22*). We have recently shown that human blood MAIT cells have the capacity to induce antibody
75 production and B cell differentiation *in vitro*, and can secrete the B cell help cytokines following
76 stimulation (*23*). Analysis of pleural effusions from tuberculosis patients revealed a population of $PD1^{High}$
77 MAIT cells secreting key B cell help cytokines (*24*). Furthermore, two recent animal studies demonstrate
78 the importance of MAIT cells in B cell help in murine autoimmunity (*25*) and mucosal vaccine immunity
79 in non-human primates (*26*).
80
81 Our aims for this study were two-fold. We first wanted to determine whether a specific subset of MAIT
82 cells are responsible for the B cell help phenotype. Our second aim was to determine *in vivo* if MAIT
83 cells were sufficient to induce antibody production and humoral immune protection in the context of
84 mucosal challenge. We found that like other innate-like T cells, MAIT cells have a Tfh like subset
85 enriched within mucosal lymphoid organs. This MAITfh population expresses classical Tfh co-

86 stimulatory markers, transcription factors, and cytokines, and is localized near B cell follicles. We further
87 show, in a murine model, that adoptively transferred MAIT cells are capable of generating microbe-
88 specific antibody responses against a mucosal bacterial pathogen in the absence of other αβ T cells.
89 Additionally, we find that in the context of mucosal challenge, MAIT cells promote increased production
90 of microbe-specific IgA antibodies and mucosal B cell differentiation. These results suggest that MAIT
91 cells have the capacity to enhance mucosal antibody mediated immunity, and thus may be a target in
92 future mucosal vaccine development.
93
94 **Results**
95 *CXCR5$^+$ MAIT cells are increased in tonsils and express higher levels of Tfh co-stimulatory markers*
96 *compared to peripheral blood.*
97 With recent evidence highlighting the ability of MAIT cells to provide B cell help, and studies showing a
98 modest population of MAIT cells within human and mouse mucosal lymphoid tissues (*39*, *41*, *42*), we
99 aimed to determine if MAIT cells had a Tfh-like subset capable of B cell help. To investigate this, we
100 used flow cytometry to analyze MAIT cell expression of classical Tfh markers in human peripheral blood
101 mononuclear cells (PBMCs) and tonsils. We obtained PBMC's from adult blood donors, and tonsils from
102 children, ages 2-16, undergoing tonsillectomy for recurrent tonsillitis or tonsillar hyperplasia. MAIT cells
103 were defined as CD3$^+$ Vα7.2$^+$ MR1-5-OPRU Tetramer$^+$ cells and gated based on a PE conjugated MR1-
104 6FP Tetramer negative control (fig S1A, S1B and Fig. 1A). Median MAIT frequency among total CD3$^+$
105 cells in tonsils was 0.23% (interquartile range (IQR) = 0.14%, 0.29%) compared to 1.03% (IQR = 0.62%,
106 1.35%) among PBMCs (Fig. 1B). We found that a higher percentage (Median=18.1%, IQR=9.2%,
107 28.6%) of tonsil MAIT cells were CXCR5$^+$ compared to PBMC MAIT cells (Median=1.74%,
108 IQR=0.37%, 2.16%, $p<0.0001$), although there was considerable variability among tonsil MAIT cells
109 (Fig. 1C and fig. S1C). To further confirm the MAIT cell phenotype, we measured expression of two C
110 type lectin receptors, CD161, a common delineator of MAIT cells (*30*), and CD69, a marker of T cell

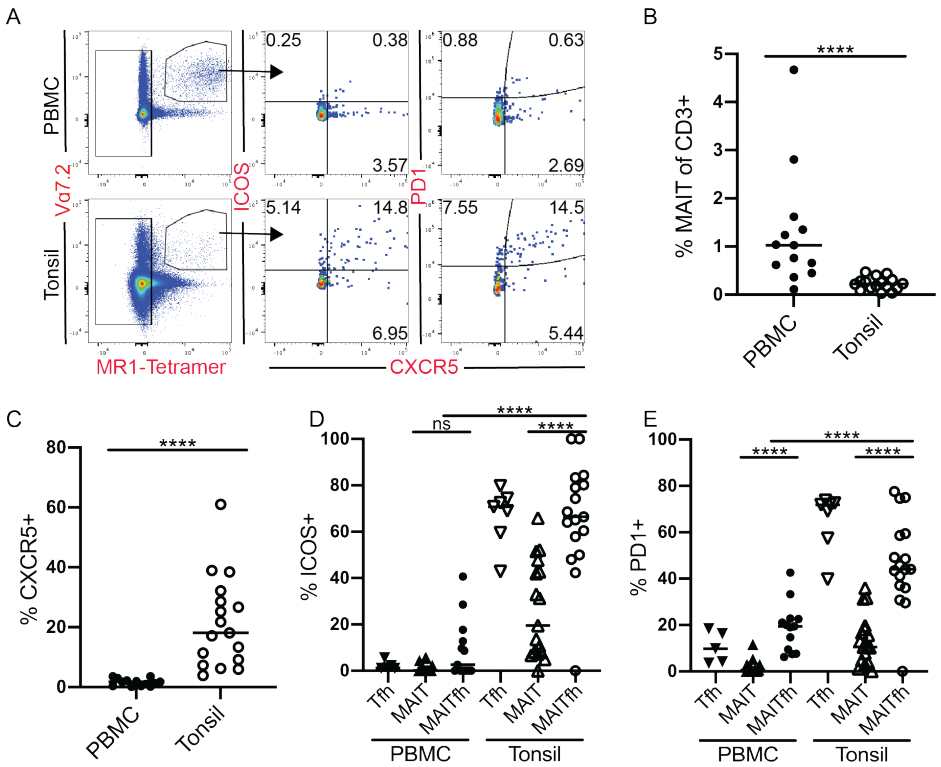

Fig. 1. Increased expression of Tfh co-stimulatory molecules in tonsil MAIT cells. (**A**) Representative FACS plots of unstimulated CD3$^+$ PBMC (top) and tonsil (bottom) cells with MAIT cell (gated in left panel) co-expression of CXCR5 with ICOS (middle) and PD1 (right). (**B**) Quantification of MAIT cell frequency as percentage of CD3$^+$. (**C**) Frequency of CXCR5$^+$ MAIT cells. Frequency of (**D**) ICOS$^+$ and (**E**) PD1$^+$ MAIT (CXCR5$^-$), MAITfh (CXCR5$^+$) and Tfh cells. Data are represented as Median from 2 pooled independent experiments. n ≥ 13. **p* < 0.05, ***p*<0.01, ****p*<0.001, *****p*<0.0001 by two-tailed Mann-Whitney *U* test

tissue residency (*43*). We found that significantly fewer CXCR5+ MAIT cells expressed CD161 in both PBMC (p<0.01) and tonsils (p<0.001) than did CXCR5- MAIT cells (fig. S2D and F). The loss of CD161 expression has been demonstrated in vitro following TCR stimulation, suggesting CXCR5+ MAIT cells may be previously activated (*44*). Despite being MR1-Tetramer+ and TRAV1-2+, we wanted to confirm that the CD161- fraction were indeed MAIT cells and therefore utilized paired TCRαβ single-cell Illumina sequencing as previously described (*45*). We sorted and single-cell sequenced CD161+ and CD161- MAIT cells (identified as live CD3$^+$ Vα7.2$^+$ MR1-Tetramer$^+$ cells) from four tonsil samples and analyzed *TRAJ* expression in *TRAV1-2* expressing wells. We found no statistically significant differences

119 in *TRAJ* expression frequency between CD161+ and CD161- MAIT cells, (fig. S3A) with the majority
120 expressing *TRAJ-33* with average frequencies of 66.3% ± 17.5 and 65.5% ± 7.9, respectively. In
121 concurrence with previous studies (*29*, *46–48*), *TRAJ-34* and *TRAJ-12* were also highly expressed in both
122 groups highlighting that these are bona fide MAIT cells. Furthermore, we found no statistically
123 significant differences in the percentages of CXCR5+ and CXCR5- MAIT cells that expressed CD69 in
124 PBMC and tonsils (fig. S2C and E), though both CXCR5+ and CXCR5- MAIT cells in the tonsils had
125 higher cell surface levels CD69 expression, indicating a tissue resident memory (Trm) phenotype. We
126 next wanted to determine if there were differences in Tfh co-stimulatory marker expression between
127 CXCR5+ and CXCR5- MAIT populations. Significantly more CXCR5+ MAIT cells in tonsils expressed
128 ICOS ($p<0.0001$) (Fig. 1D and fig S2B) than did CXCR5- MAIT cells; moreover, significantly more
129 CXCR5+ MAIT cells in both tonsils and PMBC's expressed PD1 (Fig. 1E and fig S2A) than did CXCR5-
130 MAIT cells in the same tissue. Additionally, significantly more CXCR5+ MAIT cells in tonsils expressed
131 PD1 ($p<0.0001$) and ICOS ($p<0.0001$) than did PBMC CXCR5+ MAIT cells. Notably, ICOS and PD1
132 frequency and fluorescence intensity among tonsil $CXCR5^+$ MAIT cells are similar to that seen in tonsil
133 $CD4^+$ $CXCR5^+$ (Tfh) cells (Fig.1D and 1E, and fig. S2A and S2B). In order to confirm that the
134 differences between PBMC and tonsil MAIT cells are not age dependent, we analyzed MAIT cell
135 CXCR5, ICOS and PD1 expression in 5 paired PBMC and tonsil samples from pediatric donors ages 3-15
136 (fig. S4). Similar to adult PBMC samples we found increased total MAIT frequency and decreased
137 CXCR5 expression in PMBC compared to tonsil samples (fig. S4B-C). Similar trends in ICOS and PD1
138 expression were found in the pediatric PBMC MAIT and MAITfh groups compared to the adult PBMC
139 donors supporting the use of adult PBMC samples in the following figures where low pediatric blood
140 sample volumes would limit analysis (Fig. 1D-E and fig. S4D-E). Taken together, a high proportion of
141 MAIT cells in tonsils have a $CXCR5^+$ phenotype with Tfh-like co-stimulatory markers.
142

143 *Transcriptional analyses of CXCR5$^+$ MAIT cells reveals expression of Tfh associated cytokines and*
144 *transcription factors*
145 We have previously demonstrated that peripheral blood MAIT cells can secrete B cell help cytokines IL-
146 6, IL-10 and low levels of IL-21 *in vitro* (*23*). MAIT cells are also potent producers of IFNγ (*49*), which is
147 known to have both inhibitory and activating roles in B cell development, proliferation, and antibody
148 responses (*50*). In order to investigate the transcription factor and cytokine expression of CXCR5$^+$ and
149 CXCR5$^-$ MAIT cells, we examined transcript levels of fluorescent associated cell sorted (FACS) MAIT
150 and non-MAIT CD3$^+$ T cell populations from tonsil and blood. We refer to the sorted populations, as
151 CD8$^+$ (CD8$^+$ CXCR5$^-$), Tfh (CD4$^+$ CXCR5$^+$), MAIT (MR1-Tet$^+$, Vα7.2$^+$, CXCR5$^-$), and MAITfh (MR1-
152 Tet$^+$, Vα7.2$^+$, CXCR5$^+$) (fig. S5A). To confirm our flow analysis, we assayed for *CXCR5* expression. We
153 found significant increases in *CXCR5* relative transcript levels in the MAITfh compared to the MAIT
154 groups in both PBMC's ($p<0.01$) and tonsils ($p<0.001$) (Fig. 2A). Though notably, the MAITfh group had
155 lower CXCR5 expression than the control Tfh group in both tissues. We next assayed for the Tfh lineage-
156 defining transcription factor (TF), *BCL6*. The MAITfh population within PBMCs had higher *BCL6*
157 expression compared to MAIT ($p<0.05$) and Tfh ($p<0.01$) cells. Within tonsils, MAITfh cells had higher
158 *BCL6* expression compared to Tfh ($p<0.01$) and CXCR5- MAIT ($p<0.08$) populations (Fig. 2B). In
159 comparison, analysis of canonical T cell associated TFs *RORC* (Th17) ($p<0.05$), and *TBX21* (Th1)
160 ($p<0.05$), revealed higher expression in the tonsil MAIT over the MAITfh population (Fig. 2C and D).
161 MAITfh groups had higher expression of *RORC* and *TBX21* compared to Tfh groups in PBMCs ($p<0.01$)
162 and tonsils ($p<0.01$) (Fig. 2C and D). Given that conventional Tfh cells are known to co-express TFs
163 associated with other helper T cell subsets based on lineage and environment (*51–53*), our data suggest
164 that co-expression of non-follicular helper-associated TFs in the MAITfh population may suggest
165 potential for plasticity in phenotype or differentiation from a Th1 or Th17-like subset.

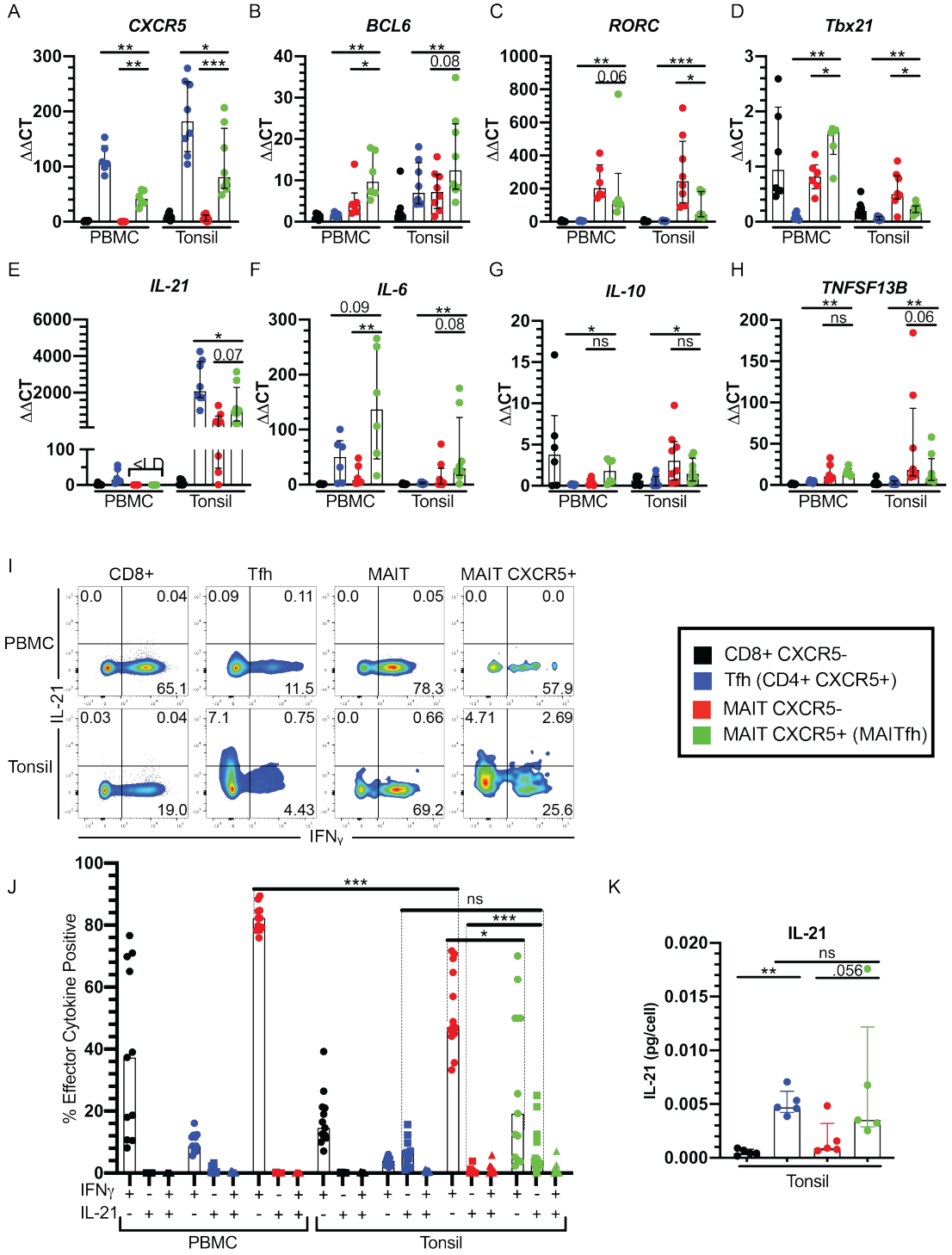
A
CXCR5
B
BCL6
C
RORC
D
Tbx21
E
IL-21
F
IL-6
G
IL-10
H
TNFSF13B
ΔΔCT
PBMC
Tonsil
I
CD8+
Tfh
MAIT
MAIT CXCR5+
IL-21
IFNγ
CD8+ CXCR5-
Tfh (CD4+ CXCR5+)
MAIT CXCR5-
MAIT CXCR5+ (MAITfh)
J
% Effector Cytokine Positive
K
IL-21
IL-21 (pg/cell)

Fig. 2. CXCR5$^+$ MAIT cells highly express B cell help cytokine IL-21. (**A**) *CXCR5*, (**B**) *BCL6*, (**C**) *RORC*, (**D**) *TBX21*, (**E**) *IL-21*, (**F**) *IL-6*, (**G**) *IL-10*, and (**H**) *TNFSF13B* qPCR data of unstimulated FAC sorted PBMC and tonsil T cell populations. Data are represented as ΔΔCt relative to an internal housekeeping gene, β-Actin, and the PBMC-CD8$^+$ CXCR5$^-$ population. Data are Median with IQR from 2 independent experiments. n=6-8. (**I**) Representative flow cytometry from PBMC and tonsil T cell populations of IL-21 and IFNγ co-expression following 6 h stimulation with PMA/Ionomycin and Brefeldin A for final 4h. (**J**) Frequency of T cell populations expressing IL-21, IFNγ or both. Data are Median with IQR from 2 pooled independent experiments. n≥11. (**K**) IL-21 ELISA following 42 h PMA/Ionomycin stimulation of FAC sorted mono-cultured T cell populations from tonsils described below. Data are Median with IQR, n=5. T cell populations described gated on live CD3+ cells are as follows: Black =CD8$^+$ CXCR5$^-$, Blue = Tfh (CD4$^+$ CXCR5$^+$), Red= MAIT (MR1-Tetramer$^+$ Va7.2$^+$) CXCR5$^-$, Green= MAIT CXCR5$^+$. Representative gating for populations found in Sup. Fig 3a. *$p < 0.05$, **$p<0.01$, ***$p<0.001$, ****$p<0.0001$ by two-tailed Mann-Whitney U test.

167 We next assayed for cytokines known to play a role in B cell differentiation or antibody production. *IL-21*
168 expression, although below the limit of detection (<LD) in PBMC MAIT and MAITfh groups, had a
169 trending increase in the tonsil MAITfh compared to the MAIT groups ($p<0.07$) (Fig. 2E). Notably,
170 although 2-5 fold lower than the tonsil Tfh group, both tonsil MAIT (median=361.3) and MAITfh
171 (Median=977.9) groups highly expressed *IL-21* relative to the tonsil CD8$^+$ CXCR5$^-$ group (Median=6.0)
172 (Fig. 2E). We found similar increases in *IL-6* expression in both PBMC and tonsil MAITfh compared to
173 MAIT and Tfh groups (Fig. 2F). Interestingly, both *TNFSF13B (BAFF)* and *IL-10* expression were
174 significantly higher in both MAIT and MAITfh groups within tonsils and PBMCs compared to Tfh cells
175 in their respective compartments (Fig. 2G and H). Taken together, CXCR5$^+$ MAIT (MAITfh) cells
176 express Tfh-associated cytokines and transcription factors at levels similar or higher than Tfh cells in their
177 respective compartments
178
179 *CXCR5$^+$ MAIT cells highly express IL-21 compared to CXCR5$^-$ MAIT cells*
180 We next wanted to investigate the relationship between IL-21 and IFNγ expression among MAIT subsets
181 as both cytokines are highly expressed and generally associated with a Tfh vs Th1 like phenotype. When
182 we stimulated PBMCs with PMA/Ionomycin, we saw a clear dichotomy between IFNγ and IL-21 positive
183 cells in all populations with very low frequency of double positive cells, and the vast majority being

184 IFNγ$^+$ (Fig. 2 I and J). MAITfh cells seemed to have a substantially lower frequency of IFNγ$^+$ cells
185 compared to conventional MAIT cells, though these data were limited by low PBMC-MAITfh cell
186 numbers, potentially biasing results. This effect was also notable in tonsils ($p<0.001$), where IFNγ
187 production in MAITfh cells was significantly reduced compared to that of MAIT cells ($p<0.05$), and IL21
188 production was significantly increased ($p<0.001$). Very few double-positive cells were recorded in either
189 population. Furthermore, the tonsil MAITfh population had a similar frequency of IL-21$^+$ cells compared
190 to conventional Tfh cells following stimulation (Fig. 2I and J). IFNγ$^+$ and IL21$^+$ frequency were low in all
191 unstimulated populations (fig. S6A-B). Conversely, when stimulated with a combination of 5-amino-6-D-
192 ribitylaminouracil (5-A-RU) and methylglyoxal to simulate MR1-dependent MAIT activation through
193 formation of the MAIT ligand, 5-OP-RU (*54*), we found minimal IL-21$^+$ MAIT or MAITfh cells and
194 statistically similar IFNγ$^+$ frequencies (fig. S7A-B). This suggests that IL-21 production by MAIT cells
195 may be MR1-independent, or dependent on alternative stimulation conditions. To confirm the IL-21
196 production capacity of MAIT cells and MAITfh cells within tonsils, we sorted MAIT (CD3$^+$ Vα7.2$^+$
197 MR1-Tetramer$^+$ CXCR5$^-$), MAITfh (CD3$^+$ Vα7.2$^+$ MR1-Tetramer$^+$ CXCR5$^+$), CD8$^+$ CXCR5$^-$ and GC
198 Tfh (CD4$^+$ CXCR5$^+$ PD1^{high}) populations, and stimulated mono-cultures of 17,000-40,000 cells with
199 PMA/Ionomycin (*55*). To account for differences in cell number per well we normalized all data to pg IL-
200 21 per cell. We found a trending increase in IL-21 production in the MAITfh over MAIT groups
201 ($p<0.056$) and no statistical difference in IL-21 production between MAITfh and GC Tfh populations
202 (Fig. 2K). Taken together, these data demonstrate the potent ability of the tonsil MAITfh population to
203 produce B-cell help cytokines and dichotomy in phenotype between classical MAIT cells and MAITfh
204 cells in both peripheral blood and tonsil tissue.
205
206 *PD1$^+$ MAIT cells localize near germinal centers within tonsils*
207 Having established that CXCR5$^+$ MAIT cells exhibit a Tfh-like phenotype *in vitro*, we next sought to
208 determine the *in vivo* spatial differences between CXCR5$^-$ and CXCR5$^+$ MAIT cells in relation to

germinal centers (GCs) in tonsil cryosections. MAIT cells were defined by co-staining of TRAV1-2 and CD161 as described in Leng et al. 2019 (*56*). Anti-IgD was used to stain naïve B cells making up the follicular mantle, and potential IgD^+ memory B cells in the marginal or superficial zone (*57*). Due to difficulties with co-staining MAIT cells and CXCR5, we used PD1 to mark MAITfh and non-MAIT GC Tfh cells (Fig. 3A). To confirm PD1 expression on Tfh cells, we stained tonsil cyrosections with anti-CD4, anti-CD3, anti-IgD and anti-PD1. We found high co-expression of $CD3^+$ $CD4^+$ cells and PD1 within tonsil GCs, while minimum PD1 expression was found in the $CD3^+$ $CD4^+$ cells outside of the follicular mantle (fig. S8A). These data suggest that GC Tfh cells can be marked by high PD1 expression. PD1 has also been used to mark GC light zone Tfh cells in human adenoid samples (*58*) and non-human primates (*59*). Furthermore, flow cytometry analysis revealed significantly higher expression of PD1 among $CXCR5^+$ (Median=44.1%, IQR=37.1%, 49.2%) vs $CXCR5^-$ (Median=10.5%, IQR=4.88%, 18.2%) MAIT cells (Fig. 1E). ImageJ was used to quantify and measure $PD1^{+/-}$ MAIT cell distance to the edge of the nearest GC, outlined in Fig. 3A (dashed white line). A total of 349 MAIT cells from n=5 tonsils were analyzed with 32% ± 15.9 being $PD1^+$. In comparison, flow results of unstimulated tonsil cells showed 38% ± 14.9 of MAIT cells to be $PD1^+$, thus confirming the ability of the immunohistochemistry imaging and quantification to assess this cell population. $PD1^+$ MAIT cells were generally located within or closely surrounding GC's with a median distance of 66.8 μm from a GC edge compared to $PD1^-$ MAIT cells with a median distance of 220.2 μm (Fig. 3B). 28.4% of $PD1^+$ MAIT cells were located within GC's and thus were recorded as 0 μm. $PD1^{High}$ expressing MAIT cells tended to localize with other $PD1^{High}$ cells within GC light zones. In contrast, $PD1^{low}$ or $PD1^-$ MAIT cells were often found outside of the IgD^{high} follicular mantle zone (Fig. 3A-yellow dashed line) and frequently in contact with IgD^{low} cells. Overall, combined with phenotypic analysis above, these data reveal $PD1^+$ (and likely $CXCR5^+$) MAIT

231 cells to be Tfh-like in their proximity to germinal centers

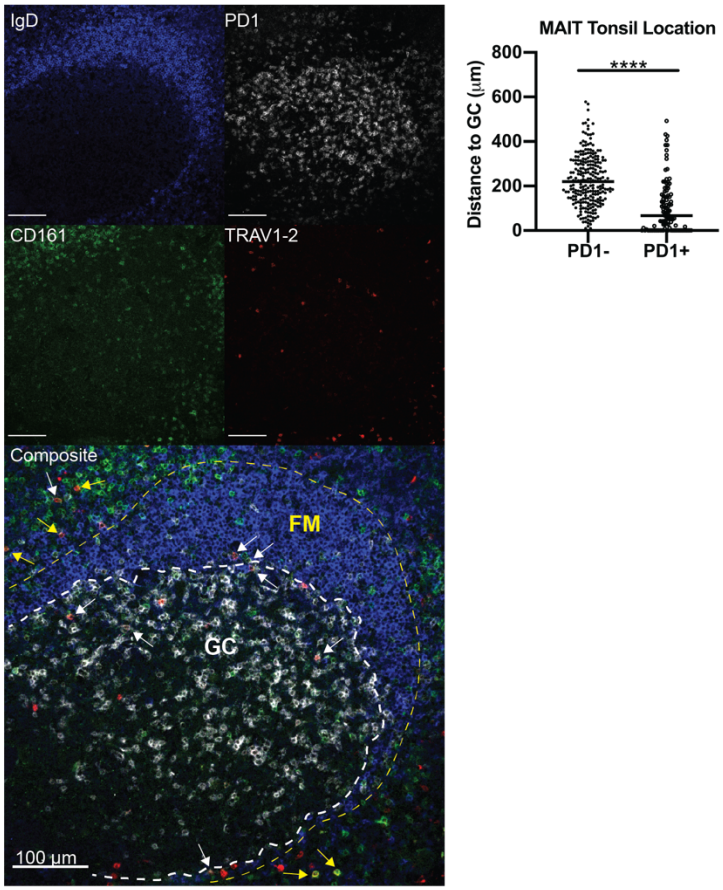

232

Fig. 3. PD1^{high} MAIT cells preferentially locate near B cell follicles. (**A**) Location of MAIT cells within tonsils. Representative immunofluorescence images from tonsil cryosections stained with anti-IgD (blue), anti-PD1 (white), anti-CD161 (green), and anti-TRAV1-2 (red) and imaged on a Leica SP8 confocal microscope with 20X objective. Enlarged composite image below with MAIT cells (TRAV1-2^{+} CD161^{+}) denoted with arrows. White arrows indicate PD1^{+} MAIT cells. Yellow arrows indicate PD1^{-} MAIT cells. White dashed line outlines germinal center (GC) highlighted by PD1^{high} cells. Yellow dashed line outlines follicular mantle (FM) highlighted by IgD^{+} naïve B cells. All scale bars represent 100 µm. (**B**) Quantification of MAIT cell distance to edge of nearest GC. Tiled images from tonsil donors were visually assessed for co-staining of CD161, TRAV1-2 and then PD1. Distance to nearest GC was then measured using ImageJ. n=359 MAIT cells were quantified (PD1^{+} = 103; PD1^{-} = 246) from n=5 tonsil donors. Data are represented as medians with dots representing single MAIT cells. *$p < 0.05$, **$p<0.01$, ***$p<0.001$, ****$p<0.0001$ by two-tailed Mann-Whitney *U* test.

233 *MAIT cells repopulate mucosal and lymphoid organs following adoptive transfer in TCRα$^{-/-}$ mice*

234 To study the sufficiency of MAIT cells to provide B cell help in the context of mucosal immune
235 responses *in vivo*, we utilized an adoptive MAIT transfer model into T*cra*^{tm1Mom}/J (TCRα$^{-/-}$) mice followed
236 by a prime-boost model of mucosal bacterial infection. Expansion of lung MAIT cells from WT C57Bl/6
237 (B6) mice using an intranasal *Salmonella* Typhimurium challenge have shown to result in MAIT cells
238 that retain function even after adoptive transfer (*40*). TCRα$^{-/-}$ mice have been successfully used in T cell
239 transfer experiments to study the B cell help potential of non-Tfh CD4 T cells without the potential
240 masking effects of classic Tfh cells (*60*). We thus adoptively transferred expanded lung MAIT cells or
241 PBS as an injection control (Sham groups) from B6 into TCRα$^{-/-}$ mice and then utilized an intranasal
242 prime-boost challenge model with live *Vibrio cholerae* O1 Inaba (*V.c*) that induces systemic and mucosal
243 LPS IgA and IgG responses (*61*) (Fig. 4A). MAIT cells have been shown to be activated during cholera
244 infection *in vivo* (*22*), and *V. cholerae* can biosynthesize riboflavin and thus can activate MAIT cells via
245 MR1 presentation of riboflavin intermediates (*62*). CXCR5 expression was present but low on D7 *S.*
246 Typhimurium expanded MAIT cells prior to adoptive transfer (fig. S10A-B). To confirm MAIT cells
247 were successfully transferred into recipient mice, we measured MAIT frequencies and total cell numbers
248 by flow cytometry of digested lung tissue and spleen (Fig. 4B and fig. S9A-C). The frequency and total
249 cell count of lung MAIT cells at Day 42 in MAIT-*V.c* and MAIT-PBS groups were statistically similar to
250 the WT- *V.c* group (Fig 4C and fig. S9B). Importantly, no MAIT cells were recorded in either Sham-*V.c*
251 or Sham-PBS group. Similar MAIT cell counts were also observed in the spleen (fig. S9C), thus
252 demonstrating WT physiologic MAIT frequencies and repopulation of various organs following adoptive
253 transfer of lung MAIT cells. Furthermore, we found no differences between all TCRα$^{-/-}$ groups in total
254 non-MAIT TCRβ^{+} T cells, thus confirming no significant expansion of contaminating non-MAIT T cells
255 following adoptive transfer (fig. S9D). We next analyzed the expression of CXCR5 in CD8 T cells, CD4
256 T cells and MAIT cells from the WT-*V.c* and MAIT cells from the MAIT-*V.c* and MAIT-PBS groups
257 (Fig. 4D and E). MAIT cells from WT-*V.c*, MAIT-*V.c* and MAIT-PBS groups, though they had decreased

258 CXCR5 MFI compared to WT CD4 T cell populations, had significantly increased CXCR5 expression
259 compared to the control CD8 T cell group in lungs, suggesting a potential mouse MAITfh population
260 (Fig. 4D and E). Taken together, we found that adoptive transfer of expanded MAIT cells into TCR$\alpha^{-/-}$
261 mice repopulates MAIT cells, including CXCR5^{+} MAIT cells in lymphoid and mucosal organs, to levels
262 similar to that of WT mice.
263
264 *MAIT cell adoptive transfer drives increase in plasmablast differentiation and memory B cell*
265 *development*
266 We next sought to determine the impact of MAIT adoptive transfer on mucosal B cell differentiation. Day
267 42 digested lung suspensions were analyzed by flow cytometry with B cells being defined as B220^{+}
268 lymphocytes (fig S11A). Interestingly, total B220^{+} cell frequency (Fig. 4F) and total B cell count per lung
269 (fig. S11B) were decreased in both the MAIT-*V.c* and MAIT-PBS groups compared to Sham-*V.c*, Sham-
270 PBS and WT-*V.c* groups. Similar decreases in IgD^{+} naïve B cell frequency were observed in MAIT
271 transfer groups (Fig. 4G), although no statistical differences were observed in total naïve B cells (fig.
272 S11C). In contrast, we found that both MAIT-*V.c* and MAIT-PBS groups had higher Memory B cell
273 (B220^{+} IgD^{-} CD27^{mid} CD38^{+} CD138^{-}) and Plasmablast (PB)/Plasma cell (PC) (B220^{low} IgD^{-} CD27^{+}
274 CD38^{+} CD138^{++}) frequency as a percentage of total B cells compared to Sham-*V.c,* Sham-PBS and WT-
275 *V.c* groups (Fig. 4H and I). Total Memory B cell count per lung was not statistically different between
276 groups with significant variability observed in the MAIT-*V.c* group (fig. S11D), though we saw a
277 trending increase in total PB/PC cell count per lung in MAIT-*V.c* compared to Sham-*V.c* (p=0.097) and
278 WT-*V.c* (p=0.179) groups (fig. S11E). Overall, these data suggest that in the absence of αβ T cells,
279 transfer of activated MAIT cells help induce B cell differentiation from naïve B cells to PB/PCs or
280 memory B cells.

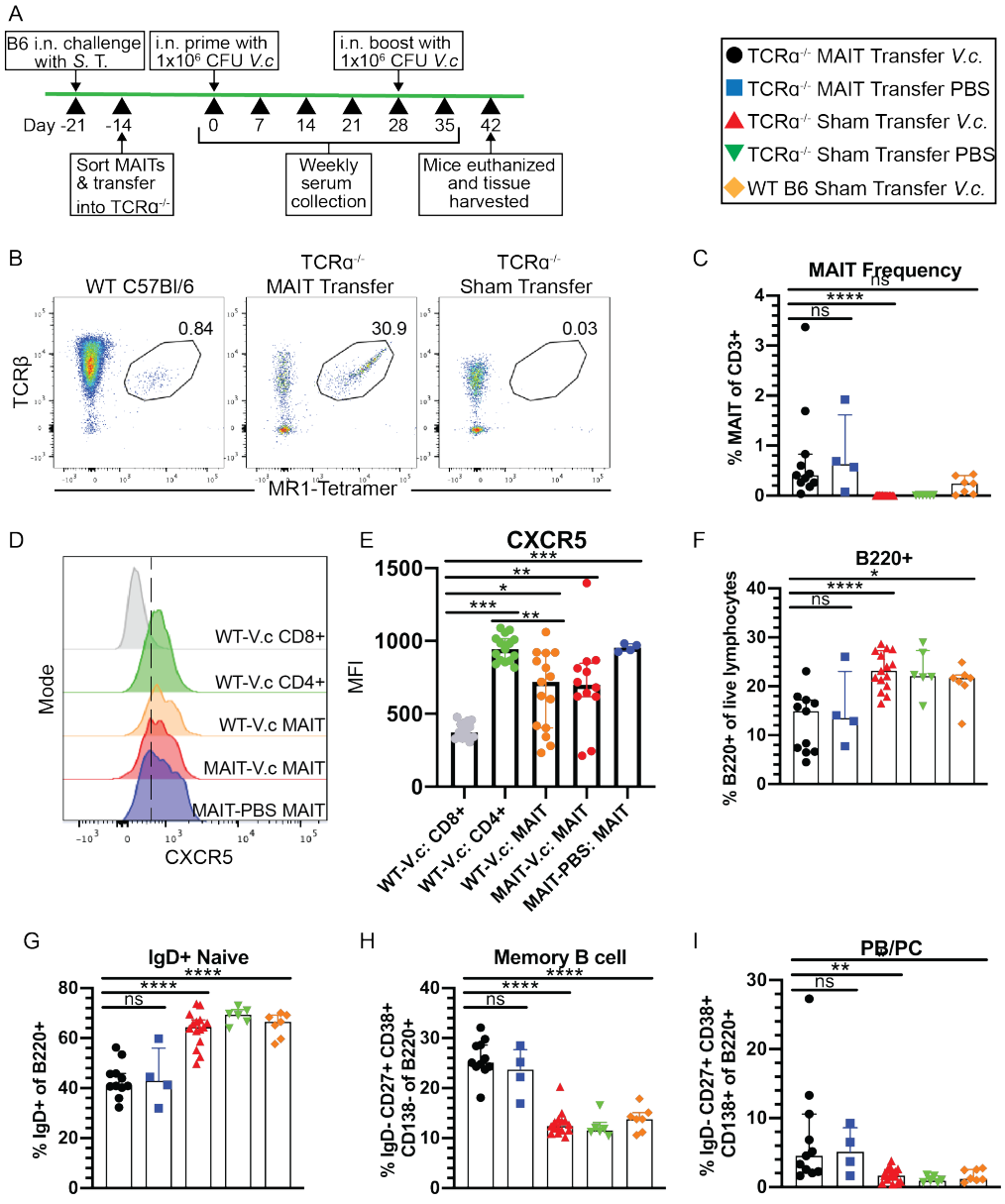
A
B6 i.n. challenge with S. T.
i.n. prime with 1x10⁶ CFU V.c
i.n. boost with 1x10⁶ CFU V.c
Day -21
-14
0
7
14
21
28
35
42
Sort MAITs & transfer into TCRα-/-
Weekly serum collection
Mice euthanized and tissue harvested
TCRα-/- MAIT Transfer V.c.
TCRα-/- MAIT Transfer PBS
TCRα-/- Sham Transfer V.c.
TCRα-/- Sham Transfer PBS
WT B6 Sham Transfer V.c.
B
WT C57Bl/6
TCRα-/- MAIT Transfer
TCRα-/- Sham Transfer
0.84
30.9
0.03
TCRβ
MR1-Tetramer
C
MAIT Frequency
% MAIT of CD3+
D
Mode
WT-V.c CD8+
WT-V.c CD4+
WT-V.c MAIT
MAIT-V.c MAIT
MAIT-PBS MAIT
CXCR5
E
CXCR5
MFI
WT-V.c: CD8+
WT-V.c: CD4+
WT-V.c: MAIT
MAIT-V.c: MAIT
MAIT-PBS: MAIT
F
B220+
% B220+ of live lymphocytes
G
IgD+ Naive
% IgD+ of B220+
H
Memory B cell
% IgD- CD27+ CD38+ CD138- of B220+
I
PB/PC
% IgD- CD27+ CD38+ CD138+ of B220+

Fig. 4. Adoptively transferred MAIT cells expand in lungs of TCRα$^{-/-}$ mice driving B cell differentiation. (**A**) MAIT adoptive transfer and *V.c* intranasal challenge time-line. (**B**) Representative FACS plots of MAIT cells (TCRβ^{+} MR1-Tetramer^{+}) from lung tissue of WT-*V.c* (left), MAIT-*V.c* (middle), and Sham-*V.c* (right) mice at Day 42 post initial *V. cholerae* challenge. (**C**) MAIT cell frequency as percentage of CD3^{+}. Representative flow cytometry histograms (**D**) and Mean fluorescence intensity quantification (**E**) of CXCR5 in WT-*V.c* CD8 T cells (grey), CD4 T cells (green) and MAIT cells (orange), MAIT-*V.c* MAIT cells (red), and MAIT-PBS MAIT cells (blue). (**F**) Frequency of B220^{+} B cells among live lymphocytes. Frequency of IgD^{+} naïve B cells (**G**), IgD^{-} CD27^{+} CD38^{+} CD138^{-} Memory B cells (**H**) and IgD^{-} CD27^{+} CD38^{+} CD138^{++} PB/PCs (**I**) as percent of B220$^{low-high}$ lymphocytes. Data are represented as Median with IQR from 4 independent experiments. n= 4-15 mice per group. **p* < 0.05, ***p*<0.01, ****p*<0.001, *****p*<0.0001 by two-tailed Mann-Whitney *U* test. Legend in black box denotes experimental groups: MAIT-*V.c* = TCRα$^{-/-}$ plus MAIT Transfer-*V.c* challenge, MAIT-PBS = TCRα$^{-/-}$ plus MAIT Transfer-PBS challenge, Sham-*V.c* = TCRα$^{-/-}$ plus Sham Transfer-*V.c* challenge, Sham-PBS = TCRα$^{-/-}$ plus Sham Transfer-PBS challenge, WT-*V.c* = WT C57Bl/6J plus Sham Transfer-*V.c* challenge.

282

283 *Increase in V. cholerae specific IgA responses following MAIT transfer*

284 *V.c*-specific antibodies in blood is a surrogate for protection against cholera (*63*, *64*). Specifically, the
285 vibriocidal assay, a measurement of complement-fixing bactericidal antibody activity, has been in use
286 since the mid twentieth century (*65*) and shown to be the best marker of protection (*66*, *67*). In addition to
287 the vibriocidal titer, cholera toxin (CT) and lipopolysaccharide (LPS) serum ELISAs have been widely
288 used to estimate cholera incidence (*67–70*). The O-specific polysaccharide (OSP) component of LPS and
289 CT are the immunodominant antigens following cholera infection (*71*). Therefore, in order to measure the
290 impact of MAIT transfer on pathogen-specific antibody kinetics we measured serum IgG, IgA, and IgM
291 antibody responses against whole *V.c*-lysate, OSP, and CT. We found comparable *V.c*-lysate IgA
292 responses in the MAIT-*V.c* and WT-*V.c* groups particularly following *V.c* re-challenge (D28), suggesting
293 development of a memory response (Fig. 5A). Day 42 endpoint ELISAs reveal a significantly higher *V.c*-
294 lysate IgA responses in the MAIT-*V.c* group compared to Sham-*V.c* (p<.0001), and MAIT-PBS (p<0.05)
295 groups, and similar responses compared to the WT-*V.c* group (p=0.58) (Fig. 5C). Importantly, minimal
296 *V.c*-lysate IgA responses were observed in the Sham-PBS group. MAIT-*V.c* and MAIT-PBS groups had
297 no significant differences in *V.c*-lysate IgG (p=0.66, Fig. 5B and D) and IgM (p=0.08, fig. S12A and B)

298 responses, despite higher compared to Sham transfer groups ($p<0.01$), thus indicating a non-specific
299 response induced by MAIT transfer. We saw a non-significant ($p=0.054$) higher OSP IgA response in the
300 MAIT-*V.c.* group compared to the Sham-*V.c* group, which can largely be attributed to high values in one
301 mouse (Fig. 5E and G). No differences were observed in OSP-IgG responses between MAIT-*V.c* and
302 Sham-*V.c* groups ($p=0.64$), Fig. 5F and H). Notably, even Sham-*V.c* TCRα-/- mice were able to mount
303 (albeit lower than WT) OSP IgG responses, indicating that a lack of T cells blunted, but did not eliminate,
304 the ability to mount an IgG response to a polysaccharide antigen, which is classically T-independent. In
305 contrast, OSP-IgM levels were similar between the MAIT-*V.c* and Sham-*V.c* ($p=0.33$), and MAIT-*V.c* and
306 WT-*V.c* groups ($p=0.11$), though were lower in the Sham-*V.c* compared to the WT-*V.c* ($p=0.03$) groups.
307 All *V.c* infected groups had higher OSP-IgM responses compared to MAIT-PBS ($p<0.05$) and Sham-PBS
308 ($p<0.01$) groups, indicating a specific but primarily T-independent response (fig. S12E and F). Overall,
309 very low levels of CT IgA and IgG were observed in all TCR$\alpha^{-/-}$ groups (Fig. 5I-L) compared to the WT-
310 *V.c* group, supporting the role of classical helper T cells in protein antigen B cell help, a response that
311 adoptive transfer of MAIT cells did not rescue. Analysis of total serum IgA revealed a highly variable but
312 substantial increase in the MAIT-*V.c* group over both Sham-*V.c* ($p<0.0001$)) and WT-*V.c* groups
313 ($p=0.01$), fig. S12H). No statistically significant changes were observed in total IgM and IgG between
314 MAIT-*V.c* and Sham-*V.c* groups (fig. S12G and I). To confirm the phenotype observed in the serum
315 corresponded to the mucosa, Bronchoalveolar lavage (BAL) fluid from a subset of MAIT-*V.c* and Sham-
316 *V.c* mice were assayed for *V.c* lysate IgA, IgG, and IgM responses. We found increased anti-lysate
317 responses in all isotypes in the MAIT-*V.c* compared to the Sham-*V.c* group which corresponded with
318 findings from serum responses (fig. S12J-L).

319

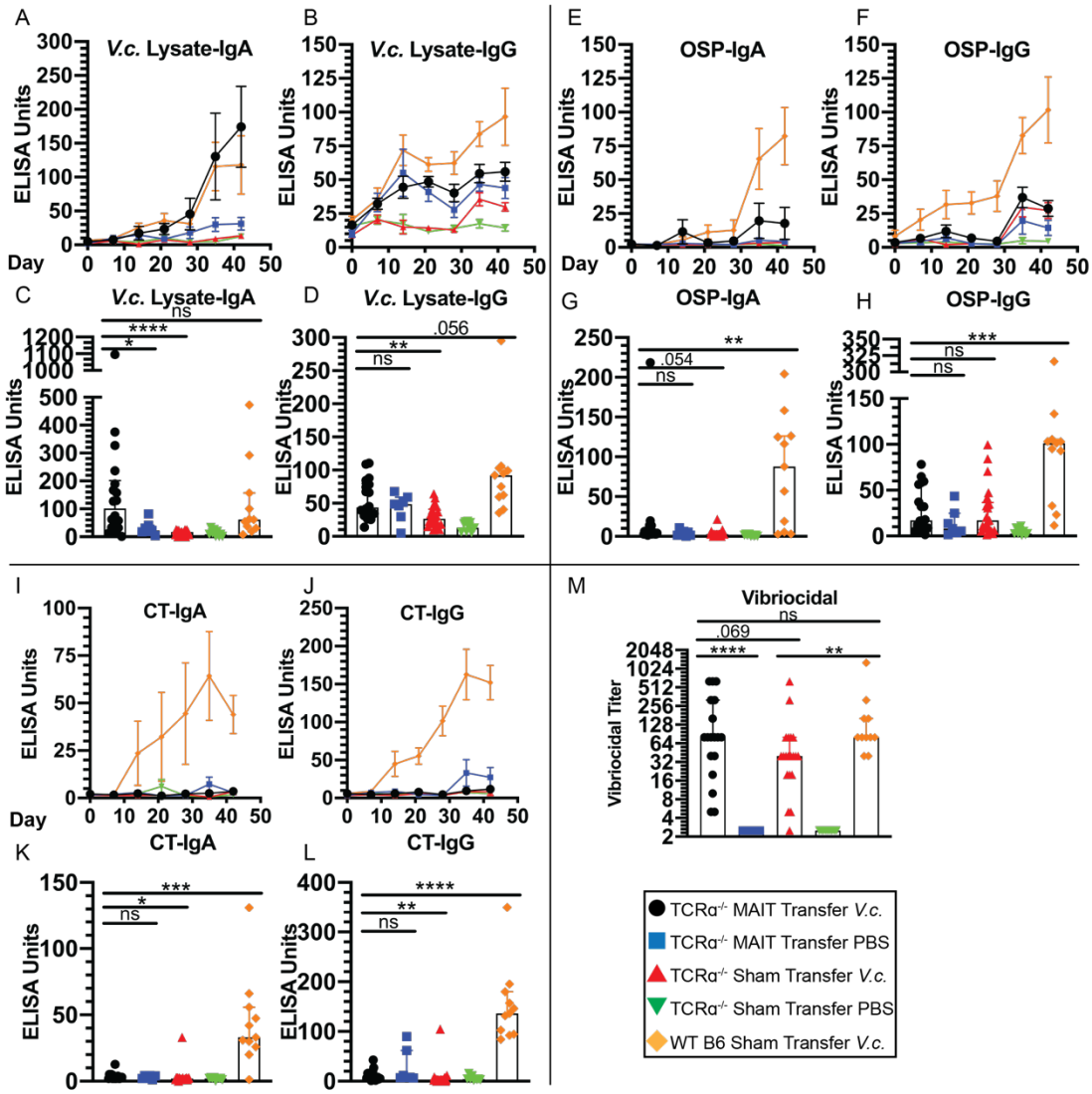

Fig. 5. MAIT cells promote *V. cholerae*-specific IgA antibody responses in TCRα$^{-/-}$ mice. Serum ELISAs against *V. cholerae* whole lysate, OSP and CT. (**A-D**) IgA and IgG *V. cholerae* lysate ELISAs from weekly cheek bleed (A & B) and Day 42 endpoint serum (C & D). (**E-H**) IgA and IgG OSP ELISAs from weekly cheek bleed (E & F) and Day 42 endpoint serum (G & H). (**I-L**) IgA and IgG CT ELISAs from weekly cheek bleed (I & J) and Day 42 endpoint serum (K & L). Data are represented as ELISA units normalized to a pooled serum positive control from WT B6 mice challenged with *V. cholerae*. (**M**) Vibriocidal titer of Day 42 endpoint serum. Data are represented as Median with IQR from 5 independent experiments. n= 6-22 mice per group. *$p < 0.05$, **$p<0.01$, ***$p<0.001$, ****$p<0.0001$ by two-tailed Mann-Whitney *U* test. Legend in black box denotes experimental groups.

320 We further utilized the vibriocidal assay to measure complement-mediated bactericidal activity, the best

321 studied and most commonly used correlate of protection from cholera in humans and a proxy for

322 protection in murine cholera challenge models (*66*, *67*, *72*). We found a trending increase in vibriocidal
323 titer in the MAIT-*V.c* group compared to the Sham-*V.c* group (p=0.069), and no difference when
324 compared to the WT-*V.c* group (Fig. 6M). Unlike the ELISAs, no background vibriocidal responses were
325 observed in the MAIT-PBS group, demonstrating the specificity of this assay. Taken together, adoptive
326 transfer of MAIT cells into T-cell deficient mice rescued deficiencies in *V. cholerae*-specific IgA and
327 promoted slight increases in vibriocidal antibody responses.
328
329 **Discussion**
330 MAIT cells are widely appreciated for their ability to respond rapidly to microbial antigens and cytokines
331 through potent production of Th1 and Th17-associated inflammatory cytokines and cytotoxic molecules.
332 Recent studies have highlighted the capacity of human MAIT cells to provide B cell help *in vitro*, and
333 promote B cell differentiation and antibody production in animal models (*23*, *25*, *26*). Despite these
334 findings, whether there remains a pre-defined MAIT subset capable of B cell help remains uncertain.
335 Additionally, many studies have detected MAIT cells within mucosal lymphoid tissues but have yet to
336 understand their role in these environments (*33*, *41*, *73*). In this study we begin to define the role of MAIT
337 cells in human mucosal lymphoid organs and uncover a novel T follicular helper-like MAIT population
338 defined by CXCR5. This MAITfh subset highly expresses PD1, ICOS, *BCL6*, and IL-21, and
339 preferentially locates near germinal centers. We further add to the body of literature proving the ability of
340 MAIT cells to provide B cell help *in vivo* through sufficiency experiments following mucosal challenge.
341 Here we show that adoptively transferred MAIT cells can rescue microbe specific IgA responses, and
342 promote B cell differentiation in the absence of other αβ T lymphocytes.
343
344 We report a subset of $CXCR5^{+}$ MAIT (MAITfh) cells that are enriched in mucosal lymphoid organs and
345 represent a small percentage of peripheral blood MAIT cells (Fig. 1C). We further report that MAITfh
346 cells highly express the B cell help co-stimulatory molecules, PD1 and ICOS, compared to $CXCR5^{-}$

347 MAIT cells (Fig 1D and E). In addition, we show high relative expression (≈30-45 fold) of *CD40L* in
348 both MAIT and MAITfh groups compared to the control CD8+ population (fig. S5B). PD1, ICOS and
349 CD40L expression are a hallmark of GC Tfh cells (*74*). PD1, although long considered a marker of T cell
350 exhaustion, has an important role in Tfh GC positioning and function (*5*). ICOS and CD40L engagement
351 with ICOS Ligand and CD40 expressed on B cells is essential for GC formation and Tfh activation (*6*, *7*).
352 CD40L is also implicated in MAIT induced maturation of dendritic cells (*75*). Based on the Tfh
353 costimulatory molecule profile, we hypothesized that MAITfh cells may share further transcriptional
354 similarities with Tfh cells. In support, we found that MAITfh cells in PBMCs have higher *BCL6*
355 expression than MAIT and Tfh cells and a trending increase in *BCL6* expression in tonsils (Fig. 2E).
356 BCL6 is considered the master regulator of the Tfh lineage (*76*) and is similarly required for iNKTfh B
357 cell help responses (*18*). Although further research into the transcriptional regulation of MAITfh cells is
358 necessary to understand the requirements for differentiation, plasticity and function, these data support a
359 B cell help transcriptional phenotype among the MAITfh subset.
360
361 We report MAITfh expression of the B cell help cytokines *IL-21*, *IL-10*, *IL-6* and *BAFF* (Fig. 2 and fig.
362 S3). Specifically, we found trending increases in *IL-21* and *IL-6* expression in MAITfh compared to
363 MAIT cells in tonsils, while *BAFF* and *IL-10* were highly expressed in both PBMC and tonsil MAIT cells
364 compared to Tfh controls (Fig. 2). IL-21 plays an important role in T dependent B cell differentiation,
365 class switching and antibody production (*77*) and together with IL-6 promotes Tfh differentiation (*78*).
366 IL-10 promotes antibody production and class switching (*79*). IL-21 expression in MAIT cells has been
367 demonstrated in low concentrations in PBMCs (*23*), and in a subset of $PD1^{High}$ $CXCR5^{-}$ MAIT cells in
368 pleural effusions from Tuberculosis patients (*24*). This study also presents a small subset of $CXCR5^{+}$
369 $PD1^{high}$ MAIT cells, though they do not investigate whether this population expressed IL-21 as well (*24*).
370 In contrast, we show that tonsil $CXCR5^{+}$ MAIT cells have a higher frequency of $IL\text{-}21^{+}$ $IFN\gamma^{-}$ cells (Fig.
371 2J) and produce more IL-21 than $CXCR5^{-}$ MAIT cells (Fig. 2K). It is unclear whether $PD1^{High}$ $CXCR5^{-}$

372 MAIT cells in pleural effusions are transcriptionally or developmentally related as potential precursors to
373 CXCR5^{+} MAIT cells found in lymphoid tissues. Furthermore, the B cell survival cytokine, BAFF, is
374 integral in T independent class switching and differentiation (*80*), and is similarly produced by iNKTfh
375 cells to promote B cell responses (*18*). Thus, it is possible MAITfh cells can aid in B cell help through
376 cognate interactions via direct MR1-TCR, co-stimulatory molecule engagement and cytokine expression,
377 or through non-cognate interactions such as promoting Tfh differentiation or licensing of dendritic cells.
378
379 We have observed that PD1^{high} MAIT cells preferentially locate within or around GCs in human tonsils
380 (Fig. 3A and B). This is noteworthy since spatial positioning of T and B cells within lymphoid tissues is
381 critical in understanding their phenotype. For instance, CXCR5^{+} PD1^{High} GC Tfh cells reside primarily in
382 the light zone of GCs where they promote affinity maturation and differentiation of GC B cells leading to
383 high affinity antibody responses (*74*). Thus, by combining imaging results with *in vitro* MAITfh
384 expression of B cell help co-stimulatory markers and cytokines (Fig. 1 and 2), we can conclude that
385 MAITfh cells share both phenotype and positioning with traditional GC Tfh cells. Thus we hypothesize
386 that this population may be involved in cognate or contact-dependent B cell help as is seen in other
387 innate-like Tfh subsets, such as iNKTfh (*12*). Though as this population is relatively small in tonsils,
388 further research will need to address the *in vivo* relevance to overall mucosal antibody production, the role
389 of MAITfh-B cell interactions in affinity maturation, and development of B cell memory.
390
391 We report that adoptive transfer of murine MAIT cells boosts pathogen-specific antibody responses in the
392 absence of other αβ T lymphocytes. We further previous work on MAIT-B cell help responses in animal
393 models (*25*, *26*), by using an adoptive transfer model to show that MAIT cells are sufficient to increase
394 functional anti-bacterial antibodies in the context of a mucosal challenge. Most notably, we show that
395 adoptive transfer of MAIT cells rescues the deficiency in *V.c*-specific IgA of infected TCRα$^{-/-}$ mice when
396 compared to infected WT mice. Examination of antibody kinetics of *V.c* specific IgA in mice receiving

397 MAIT transfer suggest a memory phenotype, based on substantial increases on Day 35 (one-week post re-
398 challenge) (Fig. 5A), and is associated with higher lung PB/PC and memory B cell frequencies (Fig. 4H
399 and I). Interestingly, we also report MAIT-*V.c* mice had significant systemic *V.c* specific IgA and total
400 IgA responses compared to Sham-*V.c* mice (Fig. 5A and fig. S12H). These data may be a result of the
401 mucosal nature of the intranasal challenge, which has shown to induce both mucosal and systemic
402 immunity in other bacterial infections (*81*). Notably, increases in total IgA in MAIT-PBS mice suggests
403 MAIT cells may specifically promote IgA class switching. In support, pulmonary MAIT cells in mice
404 have recently been shown to produce both IL-10 (*82*) and TGF1-β (*83*), key cytokines in IgA class
405 switching (*84*). Although CXCR5 staining of lung MAIT cells suggests a similar Tfh-like MAIT
406 phenotype in mice (Fig. 4D and E), limitations of available reagents for identifying murine MAIT cells by
407 IHC precludes our ability to confirm a MAITfh subset in mice. Future analysis of lung and lymph node
408 MAIT cells is necessary to confirm a MAITfh subset in mice and its potential role in IgA class switching
409 and antibody production. Given that systemic *V. cholerae* specific IgA and vibriocidal responses strongly
410 correlate with protection against subsequent cholera re-infection (*64*, *66*, *67*), these are promising data in
411 the context of mucosal vaccines, where IgA is often the primary means of protection, and development of
412 long-lasting protective memory responses is limiting (*85*). These data support further research into the
413 potential adjuvant activity of MAIT ligand administration during mucosal infection or vaccination to
414 enhance humoral immune responses.
415
416 In addition to promoting microbe-specific IgA responses, we report amplification of non-specific
417 antibodies following MAIT transfer. We report similar *V. cholerae* lysate IgG (Fig. 5B and D) and IgM
418 (fig. S11A and B), OSP (Fig. 5E-H), CT (Fig. 5I-L), total IgA (fig. S11H), and similar changes in B cell
419 subset frequencies in our MAIT-PBS and MAIT-*V.c* groups (Fig. 4F-I). Thus, regardless of *V. cholerae*
420 infection, adoptively transferred MAIT cells are promoting B cell differentiation and antibody production.
421 Similar MAIT amplification of non-specific responses were reported in non-human primates (*26*) and

422 FcγRIIB$^{-/-}$ mice (*25*). Specifically, Rahman et al. reported increased total IgM and IgG antibody
423 production and increased IgD^{-} B cells (indicating class switching) when non-human primate MAIT cells
424 were co-cultured with B cells. Murayama et. al 2019 show increases in total IgG and anti-dsDNA IgG and
425 IgA when MAIT cells were co-cultured with B cells from FcγRIIB$^{-/-}$ mice. They also report reduction in
426 anti-dsDNA IgG in MR1$^{-/-}$ (MAIT deficient) FcγRIIB$^{-/-}$ mice, though total IgG was not published. It
427 should be noted that in all studies, MAIT cells were either activated *in vitro* in direct co-culture, or *in vivo*
428 in the absence of regulatory T cells (TCRα$^{-/-}$ mice). Therefore, such responses may be a result of lack of
429 either MAIT and/or B cell regulation leading to aberrant antibody responses. This has interesting
430 consequences in the setting of mucosal immunity and in autoimmunity. In a setting of proper T and B cell
431 regulation, MAIT cells may help to promote anti-microbial responses and therefore could potentially be
432 targeted as a vaccine adjuvant. Conversely, in a dysregulated environment, such as in FcγRIIB$^{-/-}$ or TCRα^{-}
433 $^{/-}$ mice, MAIT cells may enhance aberrant antibody production against self or commensal microbes thus
434 enhancing the pro-inflammatory autoimmune state. These aberrant responses open many questions into
435 cell extrinsic MAIT regulation which remains relatively unstudied.
436
437 There are a number of limitations that need to be addressed when considering the results of this study. In
438 our human *in vitro* experiments, we primarily compare PBMCs from healthy adults ages 18+ to tonsils
439 from pediatric patients, ages 2-16, undergoing tonsillectomy. MAIT cells expand immediately after birth
440 and reach adult frequencies by approximately 10 years of age, and most reach maturity (CD45RO^{+}) by 6
441 months of age (*86*). Therefore, it is possible that age may explain low MAIT percentage in tonsil samples,
442 though analysis of 5 paired PBMC and tonsil samples pediatric donors revealed little differences in MAIT
443 frequency when compared to the healthy donor adult PBMCs (fig. S4). Limited MAIT frequency in
444 tonsils also limited our abilities to perform mechanistic analysis of our MAITfh populations. Future co-
445 culture studies with B cells and expanded MAITfh cells may be useful to understand the MAIT-B cell
446 help mechanism. Regarding our animal studies, a limitation of this study is the under sampled analysis of

447 mucosal antibody measurement, as we focused primarily on systemic responses in serum. While mucosal
448 secretory IgA (sIgA) and circulating IgA responses may differ, measurement of systemic antibodies is
449 standard practice for mucosal vaccine response testing in humans, and *V.c* specific serum IgA response
450 and vibriocidal titer strongly correlate with protection in humans (*64*, *66*, *67*). Additionally, our limited
451 analysis of BAL antibody responses correlated well with serum results. Thus, these serum responses are
452 likely relevant to mucosal protection, though lack of conclusive protective immunity via survival curves
453 or colony counts limits this finding. Secondly, our study lacks insight into the mechanism and location of
454 MAIT B cell help in our murine model. Future studies, potentially using congenic markers, are necessary
455 to address whether MAIT cells provide help within local lymph nodes, MALT or within the mucosal
456 lamina propria. Additionally, the nature of *the V. cholerae* antigens targeted by the IgA antibodies
457 remains unknown. Despite previous evidence showing association of human MAIT cells with
458 polysaccharide specific antibody responses (*22*, *35*), we found only moderate changes in OSP antibody
459 responses in our MAIT transferred mice, suggesting an alternate antigen target. Future studies are
460 necessary to address the whether MAIT cells, like other innate-like T cells, promote antibody responses to
461 specific antigen targets.
462
463 In conclusion, we identify a Tfh like MAIT population enriched near germinal centers of mucosal
464 lymphoid tissues that express cytokine and transcriptional profiles consistent with B cell help. In addition,
465 we show in an animal model that MAIT cells are sufficient to rescue pathogen-specific IgA antibody
466 responses following mucosal challenge in the absence of other classical T cells. Our work strengthens a
467 growing body of evidence supporting the capacity of MAIT cells to aid in B cell help and antibody
468 mediated immunity, and support the expanding phenotypic heterogeneity of MAIT cells (*87*). As MAIT
469 cells are enriched at the mucosa and can be activated with specific ligands, we hypothesize that they may
470 be a promising target to enhance mucosal vaccines.

471 **Materials and Methods**

472 *Peripheral blood and tonsil collection*

473 Healthy adult blood was collected from residual leukocyte packs following blood donation (ARUP,
474 Sandy, UT), and PBMC's were isolated by density gradient centrifugation (Lymphoprep, StemCell
475 Technologies). Residual palatine tonsil samples were acquired from pediatric patients, ages 2-16,
476 undergoing routine tonsillectomies for tonsillar hyperplasia or recurrent tonsillitis. All tonsil samples
477 were stored on ice in complete media (RPMI 1640 with 10% FBS, 1% penicillin/streptomycin, and 15
478 mM HEPES) (R10) and processed within 2 hours of surgery. 1 cm x 1 cm pieces were cut and frozen in
479 O.C.T. Compound (Fisher) at -80°C for later use. The remaining tonsil tissue was minced in media and
480 dissociated using a 100 μM cell strainer. Tonsil mononuclear cells were isolated by density gradient
481 centrifugation (Lymphoprep, StemCell Technologies). PBMC's from pediatric donors were obtained
482 during surgery with informed consent granted by a parent/guardian. PBMC and tonsil mononuclear cells
483 were frozen in media containing 25% FBS and 10% DMSO at -80°C for later use. All human samples
484 were de-identified prior to receipt, and the research protocol was deemed exempt by the University of
485 Utah Institutional Review Board (Protocol 100683).

486

487 *Flow cytometry and cell sorting*

488 Prior to surface staining, human and mouse single cell suspensions were labeled with Fixable Viability
489 Dye eFluor 780 (eBioscience) according to manufacturer's protocol to delineate live cells. Cells were
490 washed and incubated with fluorochrome conjugated antibodies for 20 min at room temperature (RT).
491 Mouse cells were incubated in anti-mouse CD16/CD132 (Fc block) for 15 minutes prior to surface
492 staining. Mouse and human MR1-Tetramers (NIH Tetramer Core) diluted 1:400 were added to surface
493 stain. Prior to mouse MR1-Tetramer staining, cells were incubated for 15 minutes with unlabeled i6FP-
494 Tetramer (NIH Tetramer Core) to minimize non-specific binding. For intracellular cytokine staining, cells
495 were fixed and permeabilized using Foxp3/Transcription Factor Staining Buffer set (eBioscience)

496 according to manufacturer's protocol and incubated with fluorochrome conjugated antibodies for 40 min
497 at RT. Cells were analyzed using BD LSR Fortessa or Cytek Aurora for phenotypic analyses, or Aria II
498 (BD Biosciences) for cell sorting. The following monoclonal antibodies to human were used : CD3-
499 AF700 (clone OKT3), CD8-FITC/BV605 (cloneSK1, TCR Vα7.2-BV711/PE-Cy7 (clone 3C10), PD1-
500 BV605/AF700 (clone EH12-2H7), ICOS-PerCP-Cy5.5/BV605 (clone C398.4A), CXCR5-PE-Cy7/APC
501 (clone J252D4), IL-21-APC (clone 3A3-N2), IFNγ-BV421 (clone B27), IL-6-FitC (clone MQ2-13A5),
502 IL-10-PerCP-Cy5.5 (clone JES2-9D7), CD161-AF488 (clone HP-3610) (Biolegend), CD4-BUV496
503 (clone SK3), CD3-BUV395 (clone SK7) (BD Biosciences). The following monoclonal antibodies to
504 mouse were used: CD3-PE-Dazzle594 (clone 17A2), TCRβ-BV421 (clone H57-597), CXCR5-BV605
505 (clone L138D7), CD44-BV650 (clone IM7), TCRγδ-PE-Cy7 (clone GL3), CD8-APC (clone 53-6.7),
506 CD45R-PE-Cy5 (clone RA3-6B2), IgD-BV510 (clone 11-26c.2a), CD138-BV605 (clone 281-2), CD38-
507 PE-Cy7 (clone 90, CD27-APC (clone LG-3A10) (Biolegend), CD4-FITC (clone GK1.5) (Tonbo
508 Biosciences).
509
510 *In vitro stimulation assays*
511 For flow cytometry intracellular cytokine staining, 1-2 x 10^6 mononuclear cells isolated from blood or
512 tonsil samples were cultured in a round bottom 96 well plate at 37°C 5% CO_2 in R10 media for 6 hours
513 with or without 200 ng/ml phorbol myristate acetate (PMA) and 1.0 μg/ml Ionomycin (Sigma-Aldrich) or
514 0.5 μM/ml 5-amino-6-D-ribitylaminouracil (5-A-RU) (courtesy of Jeffrey Aubé, UNC) and 50 μM/ml
515 Methylglyoxal (Sigma). Brefeldin A Solution (Biolegend) was added at 1X for the final 4 hours. For
516 measurement of IL-21 production, tonsil mononuclear cells were sorted into $CD8^+$ $CXCR5^-$, $CD4^+$
517 $CXCR5^+$ $PD1^{High}$, MR1-Tet^+, $V\alpha7.2^+$, $CXCR5^-$, MR1-Tet^+, $V\alpha7.2^+$, $CXCR5^+$ populations and $4x10^4$ cells
518 in R10 media were cultured in a round bottom 96 well plate for 48 h with 20 ng/ml PMA and 1.0 μg/ml
519 Ionomycin as described in Shen et al (*55*). Plates were centrifuged and cell supernatant was isolated for
520 ELISAs.

521

522 *qRT-PCR*

523 PBMC and tonsil $CD8^+$ $CXCR5^-$, $CD4^+$ $CXCR5^+$, MR1-Tet^+ $V\alpha7.2^+$ $CXCR5^-$, MR1-Tet^+ $V\alpha7.2^+$

524 $CXCR5^+$ cells were sorted into TRIzol Reagent (Qiagen). Total RNA was isolated using the RNeasy

525 Micro kit and cDNA synthesized a High-Capacity cDNA Reverse Transcription Kit (Applied

526 Biosystems). Targeted qPCR was performed using the QuantStudio 6 Real-Time PCR system using the

527 following Taqman Primers (Applied Biosystems): BCL6 (Hs00153368_m1), Tnfsf13b

528 (Hs00198106_m1), IL6 (Hs00174131_m1), IL10 (Hs00961622_m1), IL21 (Hs00222327_m1), TNFα

529 (Hs00174128_m1), TGFB1 (HS00998133_m1), Tcf7 (Hs01556515_m1), Tbx21 (Hs00894392_m1),

530 Runx3 (Hs01091094_m1), Rorc (Hs01076112_m1), Perforin (Hs00169473_m1), Pdcd1

531 (Hs01550088_m1), Il17a (Hs00174383_m1), Ifnγ (Hs00989291_m1), Icos (Hs00359999_m1), Gzmb

532 (Hs00188051_m1, Cxcr5 (Hs00173527_m1), Cd40l (Hs00163934_m1), Cd38 (Hs01120071_m1),

533 Blimp1 (Hs00153357_m1), Ascl2 (Hs00270888_s1), ActB (Hs99999903_m1).

534

535 *Single cell TCR sequencing*

536 MAITs from PBMC's and tonsils were single cell sorted using the Aria II cell sorter (BD Biosciences)

537 directly into One Step RT-PCR reaction mix (NEB) loaded in MicroAmp Optical 96-well reaction plates

538 (Applied Biosystems). MAITs were defined as $CD3^+$ $V\alpha7.2^+$ MR1-$Tetramer^+$ cells and sorted based on

539 CD161 expression. Following reverse transcription and preamplification reaction, a series of three nested

540 PCR's were run using primers for TCR sequence and gene expression as described (*45*). Subsequent

541 sequencing data analysis was performed as described (*45*).

542

543 *ELISAs and Vibriocidal assay*

544 IL-21 concentration from tonsil mono-cultures was measured using Human IL-21 ELISA MAX Deluxe

545 kit (Biolegend) according to manufacturer's protocol. Serum *V.c* Lysate, OSP:BSA and CT ELISAs were

546 performed as follows. Nunc Maxisorp flat bottom 96 well plates (Invitrogen) were coated with *V.c* Lysate
547 or OSP:BSA (gift from Dr. Edward Ryan (Massachusetts General Hospital, Boston, MA) (1.0 μg/ml) in
548 PBS and incubated overnight at 4°C. For CT ELISAs, Nunc plates were first coated with
549 Monosialoganglioside G_{M1} (Sigma-Aldrich) (1.0 μg/ml) in 50mM carbonate buffer overnight at 4°C.
550 Plates were subsequently blocked with 1% bovine serum albumin (BSA) (Sigma-Aldrich) and incubated
551 overnight with CT (Sigma-Aldrich) (2.5 μg/ml) in carbonate buffer. All plates were then blocked with 1%
552 BSA and 25 μl of mouse serum diluted 1:10 in 0.1% BSA-0.5% Tween 20 in PBS (BSA-PBST) was
553 added for 2 hours. Plates were incubated with anti-mouse IgG (Invitrogen), IgA (Invitrogen), or IgM (Life
554 Technologies) HRP conjugate diluted 1:1000 in BSA-PBST for 2 hours. 100 μl of TMB substrate
555 (Thermo Fisher) was added and plates were immediately read kinetically at 405 nm (7 min x 1 min
556 intervals) using plate reader (Biotek). ELISA measurements were recorded as max interval slope and
557 normalized to pooled positive mouse sera included on each plate. Total Ig ELISAs were performed as
558 described above except Nunc plates were pre-coated with anti-mouse IgA (clone RMA1), anti-mouse IgG
559 (clone Poly 4053), or anti-mouse IgM (clone RMM-1) (Biolegend) and standard curves were generated
560 using 2-fold dilutions of purified Mouse IgA, IgM and IgG (Southern Biotech). Plates were incubated
561 with corresponding anti-mouse HRP antibodies and TMB substrate was neutralized after 10 min with 0.2
562 N HCl. Plates were read at 605 nm and concentrations were calculated based on the standard curve.
563 Vibriocidal titer was measured as described (*88*). *Vibrio cholerae* serotype 01 Strain El Tor Inaba N16961
564 grown in LB media was used as target organism for assay, and serum samples were diluted to a starting
565 concentration of 1:5.
566
567 *Immunofluorescence staining*
568 Unfixed pediatric tonsil samples frozen in OCT medium were cut into 9μm thick sections using a cryostat
569 (Leica) and stored at -80°C. Tonsil sections were brought to room temperature and then fixed at -20°C for
570 10 min in pre-cooled 50:50 Acetone:Methanol solution. Sections were dried and then rehydrated in PBS

571 for 5 min with gentle shaking. The sections were then blocked in 2% normal mouse serum (Invitrogen)
572 for 1 hour and subsequently stained overnight at 4°C with mouse anti-human TCR Vα7.2-PE (Clone
573 3C10, Biolegend), mouse anti-human CD161-AF488 (Clone NKR-P1A, Biolegend), mouse anti-human
574 IgD-BV421 (Clone IA6-2, Biolegend) and mouse anti-human PD1-APC (Clone EH1202H7, Biolegend)
575 all diluted 1:100. Sections were washed 3x in PBS and mounted using ProLong Gold Antifade Mounting
576 media (Thermo Fisher). Full tonsil cross section images were acquired using the Leica Sp8 Confocal
577 microscope and then processed and analyzed using ImageJ.
578
579 *Bacterial culture and V. cholerae lysate preparation*
580 The attenuated *Salmonella* Typhimurium strain BMM50 was a gift from Dr. Stephen McSorely (UC
581 Davis, Davis, CA). BMM50, like previously published *S.* Typhimurium BRD509 (*39*), has a deleted *aroA*
582 gene and intact riboflavin pathway. *Vibrio cholerae* serotype 01 Strain El Tor Inaba N16961 was a gift
583 from Dr. Edward Ryan (Massachusetts General Hospital, Boston, MA). All strains were inoculated from
584 single colonies into Luria Bertani (LB) broth shaking at 220 RPM 37°C overnight. They were then
585 subcultured 1:10 in fresh LB and incubated for 3-4 hours shaking at 37°C until log phase was reached.
586 Cultures were washed 2x in sterile PBS and normalized to 0.1 OD600 using a microplate absorbance
587 spectrophotometer (BioRad). *V. cholerae* at 0.1 OD600 was used as inoculum for intranasal challenge
588 model. *S.* Typhimurium BMM50 was diluted 1:10 with PBS to an OD600 of 0.01 for adoptive transfer
589 inoculum. Inoculums ranged from $1x10^6$-$1x10^7$ colony forming units (CFU) confirmed by plate counts. *V.*
590 *cholerae* lysate for ELISAs was prepared as follows. *V. cholerae* was cultured from a single colony in LB
591 broth shaking at 220 RPM 37°C overnight. *V. c* culture was then pelleted and washed 3x with cold sterile
592 PBS. Following resuspension in PBS, sample was sonicated at 40% power 4 x 1 min intervals, keeping on
593 ice for 1 minute between runs. Sonicated sample was then centrifuged at 15000 rpm x 10 min at 4°C, and
594 the supernatant removed and sterilized using 0.2 µm syringe filter (Thermo Fisher). Protein content was
595 measured using 260/280 absorbance ratio with Take3 Micro-Volume Plate reader (BioTek)

596

597 *Mice*

598 T*cra*^{tm1Mom}/J mice (*89*) (on a B6 background) were obtained from The Jackson Laboratory (Bar Harbor,
599 ME) and bred at the University of Utah Comparative Medicine Center mouse facility. WT C57BL/6J
600 mice were obtained directly from The Jackson Laboratory prior to the start of the experiment. 6-10-week-
601 old female and male mice were used in adoptive transfer studies. All mice were housed under specific
602 pathogen-free conditions. Experiments were performed in strict accordance with the NIH guide for the
603 Care and Use of Laboratory animals and institutional guidelines for animal care at the University of Utah
604 under approved protocol #17-01011.

605

606 *Adoptive transfer*

607 Adoptive transfer of pulmonary MAIT cells was adapted from protocol described (*40*). C57BL/6 mice
608 were infected i.n. with 10^6 CFU *S.* Typhimurium BMM50 suspended in 50 µl sterile PBS (25 µl per
609 nares). Mice were rested for 7 days to allow for MAIT expansion, in which mice were weighed daily and
610 evaluated for signs of clinical pneumonia symptoms (respiratory distress, inactivity, ruffled fur, hunched
611 posture). Mice with loss of >20% of body weight and/or severe clinical symptoms were euthanized. On
612 day 7, mice were euthanized and the lungs were perfused with 10 mls of PBS through the heart and then
613 removed. Single cells suspensions of lungs were prepared using the gentleMacs Lung Dissociation kit,
614 mouse (Miltenyi Biotech) according to the manufacturer's protocol. Red blood cells were lysed using
615 ACK Lysis buffer (Thermo Fisher), and single cell suspensions were stained and sorted using the BD
616 FACS Aria II. MAIT cells were defined as live $CD3^+$ $B220^-$ $TCR\gamma\delta^-$ $CD44^{high}$ $TCR\beta^+$ MR1-Tetramer$^+$
617 lymphocytes. Approximately $5x10^4$ - $1x10^5$ MAIT cells were sorted per mouse. 10^5 MAIT cells
618 suspended in 100 µl was transferred via retroorbital injections into lightly anesthetized mice. Transferred
619 mice were monitored to confirm recovery following injections, and rested for 2 weeks to allow for MAIT
620 expansion before use in intranasal challenge model.

621

622 *Intranasal challenge model*

623 The following protocol was adapted from Nygren et al (*61*) to induce *V. cholerae* specific antibody
624 responses through a prime-boost live bacterial model. In brief, on Day 0 mice were anesthetized using
625 isoflurane and infected i.n. with 10^6-10^7 CFU *V. cholerae* 01 Biotype El Tor Serotype Inaba suspended in
626 50 µl sterile PBS (25 µl per nares). Mice were monitored for 7 days post infection for weight loss and
627 clinical signs of pneumoniae (outlined above). Mice with loss of >20% of body weight and/or severe
628 clinical symptoms were euthanized. Mice were subsequently re-challenged on Day 28 using the above
629 protocol. Blood samples were collected weekly, prior to infections on Day 0 and 28, from submandibular
630 bleeds on lightly isoflurane anesthetized mice. Blood serum was isolated using BD Microtainer SST tubes
631 (BD Biosciences) according to the manufacturer's protocol. On Day 42 (2 weeks post re-challenge), mice
632 were euthanized using a bell jar and isoflurane. Blood was collected immediately via cardiac puncture and
633 serum isolated. Lungs were perfused and single cell suspensions were processed as described above.
634 Spleens were excised, ground through 70 µm filters in cold R10 media. Red blood cells were lysed using
635 ACK Lysis Buffer (Thermo Fisher). 1-2x10^6 cells from lung and spleen cell suspensions were stained
636 with fluorochrome conjugated antibodies for flow cytometric analyses.

637

638 *Statistical analysis*

639 All statistical tests were performed using Prism version 8.4.2 (GraphPad Software, La Jolla, CA, USA).
640 Differences were compared using two-tailed Mann Whitney *U* tests, or Multiple t tests comparisons
641 accounting for False Discoveries using the Benjamini, Krieger and Yekutieli correction as indicated.
642 Graphs were created using Prism or R (Vienna, Austria) and the graphing package ggplot2 (H. Wickham,
643 Springer-Verlag, NY, USA).

644

645

646 **References**

647 1. C. Gutzeit, G. Magri, A. Cerutti, Intestinal IgA production and its role in hot-microbe interaction.
648 *Immunol. Rev.* **260**, 76–85 (2014).

649 2. O. Pabst, E. Slack, IgA and the intestinal microbiota: the importance of being specific. *Mucosal*
650 *Immunol.* **13**, 12–21 (2020).

651 3. S. Hardtke, L. Ohl, R. Förster, Balanced expression of CXCR5 and CCR7 on follicular T helper
652 cells determines their transient positioning to lymph node follicles and is essential for efficient B-
653 cell help. *Blood*. **106**, 1924–1931 (2005).

654 4. H. Qi, T follicular helper cells in space-time. *Nat. Rev. Immunol.* **16**, 612–625 (2016).

655 5. J. Shi, S. Hou, Q. Fang, X. Liu, X. Liu, H. Qi, PD-1 Controls Follicular T Helper Cell Positioning
656 and Function. *Immunity*. **49**, 264-274.e4 (2018).

657 6. A. Tafuri, A. Shahinian, F. Bladt, S. K. Yoshinaga, M. Jordana, A. Wakeham, L. M. Boucher, D.
658 Bouchard, V. S. F. Chan, G. Duncan, B. Odermatt, A. Ho, A. Itie, T. Horan, J. S. Whoriskey, T.
659 Pawson, J. M. Penninger, P. S. Ohashi, T. W. Mak, ICOS is essential for effective T-helper-cell
660 responses. *Nature*. **409**, 105–109 (2001).

661 7. G. Van Kooten, J. Banchereau, CD40-CD40 ligand. *J. Leukoc. Biol.* **67**, 2–17 (2000).

662 8. K. Ozaki, R. Spolski, C. G. Feng, C. F. Qi, J. Cheng, A. Sher, H. C. Morse, C. Liu, P. L.
663 Schwartzberg, W. J. Leonard, A critical role for IL-21 in regulating immunoglobulin production.
664 *Science (80-.).* **298**, 1630–1634 (2002).

665 9. G. Galli, P. Pittoni, E. Tonti, C. Malzone, Y. Uematsu, M. Tortoli, D. Maione, G. Volpini, O.
666 Finco, S. Nuti, S. Tavarini, P. Dellabona, R. Rappuoli, G. Casorati, S. Abrignani, Invariant NKT
667 cells sustain specific B cell responses and memory. *Proc. Natl. Acad. Sci. U. S. A.* **104**, 3984–9
668 (2007).

669 10. E. Tonti, G. Galli, C. Malzone, S. Abrignani, G. Casorati, P. Dellabona, NKT-cell help to B
670 lymphocytes can occur independently of cognate interaction. *Blood*. **113**, 370–376 (2009).

671 11. S. T. Scanlon, S. Y. Thomas, C. M. Ferreira, L. Bai, T. Krausz, P. B. Savage, A. Bendelac,
672 Airborne lipid antigens mobilize resident intravascular NKT cells to induce allergic airway
673 inflammation. *J. Exp. Med.* **208**, 2113–2124 (2011).
674 12. E. A. Leadbetter, M. Brigl, P. Illarionov, N. Cohen, M. C. Luteran, S. Pillai, G. S. Besra, M. B.
675 Brenner, NK T cells provide lipid antigen-specific cognate help for B cells. *Proc. Natl. Acad. Sci.*
676 **105**, 8339–8344 (2008).
677 13. P. Barral, J. Eckl-Dorna, N. E. Harwood, C. De Santo, M. Salio, P. Illarionov, G. S. Besra, V.
678 Cerundolo, F. D. Batista, B cell receptor-mediated uptake of CD1d-restricted antigen augments
679 antibody responses by recruiting invariant NKT cell help in vivo. *Proc. Natl. Acad. Sci.* **105**,
680 8345–8350 (2008).
681 14. I. L. King, A. Fortier, M. Tighe, J. Dibble, G. F. M. Watts, N. Veerapen, A. M. Haberman, G. S.
682 Besra, M. Mohrs, M. B. Brenner, E. A. Leadbetter, Invariant natural killer T cells direct B cell
683 responses to cognate lipid antigen in an IL-21-dependent manner. *Nat. Immunol.* **13**, 44–50
684 (2012).
685 15. E. Tonti, M. Fedeli, A. Napolitano, M. Iannacone, U. H. von Andrian, L. G. Guidotti, S.
686 Abrignani, G. Casorati, P. Dellabona, Follicular Helper NKT Cells Induce Limited B Cell
687 Responses and Germinal Center Formation in the Absence of CD4 + T Cell Help . *J. Immunol.*
688 **188**, 3217–3222 (2012).
689 16. H. B. Shah, S. K. Joshi, M. L. Lang, CD40L-null NKT cells provide B cell help for specific
690 antibody responses. *Vaccine*. **29**, 9132–9136 (2011).
691 17. P. Rampuria, G. A. Lang, T. S. Devera, C. Gilmore, J. D. Ballard, M. L. Lang, Coordination
692 between T helper cells, iNKT cells, and their follicular helper subsets in the humoral immune
693 response against *Clostridium difficile* toxin B. *J. Leukoc. Biol.* **101**, 567–576 (2017).
694 18. P. P. Chang, P. Barral, J. Fitch, A. Pratama, C. S. Ma, A. Kallies, J. J. Hogan, V. Cerundolo, S. G.
695 Tangye, R. Bittman, S. L. Nutt, R. Brink, D. I. Godfrey, F. D. Batista, C. G. Vinuesa,

696 Identification of Bcl-6-dependent follicular helper NKT cells that provide cognate help for B cell
697 responses. *Nat. Immunol.* **13**, 35–43 (2012).
698 19. N. Caccamo, L. Battistini, M. Bonneville, F. Poccia, J. J. Fournie, S. Meraviglia, G. Borsellino, R.
699 A. Kroczek, C. La Mendola, E. Scotet, F. Dieli, A. Salerno, CXCR5 Identifies a Subset of V 9V 2
700 T Cells which Secrete IL-4 and IL-10 and Help B Cells for Antibody Production. *J. Immunol.* **177**,
701 5290–5295 (2006).
702 20. R. R. Bansal, C. R. Mackay, B. Moser, M. Eberl, IL-21 enhances the potential of human γδ T cells
703 to provide B-cell help. *Eur. J. Immunol.* **42**, 110–119 (2012).
704 21. R. M. Rezende, A. J. Lanser, S. Rubino, C. Kuhn, N. Skillin, T. G. Moreira, S. Liu, G. Gabriely,
705 B. A. David, G. B. Menezes, H. L. Weiner, γδ T cells control humoral immune response by
706 inducing T follicular helper cell differentiation. *Nat. Commun.* **9** (2018), doi:10.1038/s41467-018-
707 05487-9.
708 22. D. T. Leung, T. R. Bhuiyan, N. S. Nishat, M. R. Hoq, A. Aktar, M. A. Rahman, T. Uddin, A. I.
709 Khan, F. Chowdhury, R. C. Charles, J. B. Harris, S. B. Calderwood, F. Qadri, E. T. Ryan,
710 Circulating mucosal associated invariant T cells are activated in Vibrio cholerae O1 infection and
711 associated with lipopolysaccharide antibody responses. *PLoS Negl. Trop. Dis.* **8**, e3076 (2014).
712 23. M. S. Bennett, S. Trivedi, A. S. Iyer, J. S. Hale, D. T. Leung, Human mucosal-associated invariant
713 T (MAIT) cells possess capacity for B-cell help. *J. Leukoc. Biol.* **102**, 1261–1269 (2017).
714 24. J. Jiang, Z. Cao, PD-1-expressing MAIT cells from patients with tuberculosis exhibit elevated
715 production of CXCL13, 1–15 (2020).
716 25. G. Murayama, A. Chiba, H. Suzuki, A. Nomura, T. Mizuno, T. Kuga, S. Nakamura, H. Amano, S.
717 Hirose, K. Yamaji, Y. Suzuki, N. Tamura, S. Miyake, A Critical Role for Mucosal-Associated
718 Invariant T Cells as Regulators and Therapeutic Targets in Systemic Lupus Erythematosus. *Front.*
719 *Immunol.* **10**, 2681 (2019).
720 26. M. A. Rahman, E. Ko, F. Bhuyan, G. Enyindah-asonye, R. Hunegnaw, S. H. Hait, C. J. Hogge, D.

721 J. Venzon, T. Hoang, M. Robert-guroff, Mucosal-associated invariant T (MAIT) cells provide B-
722 cell help in vaccinated and subsequently SIV- infected Rhesus Macaques. *Sci. Rep.*, 1–17 (2020).
723 27. F. Tilloy, E. Treiner, S. H. Park, C. Garcia, F. Lemonnier, H. de la Salle, A. Bendelac, M.
724 Bonneville, O. Lantz, An invariant T cell receptor alpha chain defines a novel TAP-independent
725 major histocompatibility complex class Ib-restricted alpha/beta T cell subpopulation in mammals.
726 *J. Exp. Med.* **189**, 1907–21 (1999).
727 28. R. Reantragoon, A. J. Corbett, I. G. Sakala, N. A. Gherardin, J. B. Furness, Z. Chen, S. B. G.
728 Eckle, A. P. Uldrich, R. W. Birkinshaw, O. Patel, L. Kostenko, B. Meehan, K. Kedzierska, L. Liu,
729 D. P. Fairlie, T. H. Hansen, D. I. Godfrey, J. Rossjohn, J. McCluskey, L. Kjer-Nielsen, Antigen-
730 loaded MR1 tetramers define T cell receptor heterogeneity in mucosal-associated invariant T cells.
731 *J. Exp. Med.* **210**, 2305–20 (2013).
732 29. M. Lepore, A. Kalinicenko, A. Colone, B. Paleja, A. Singhal, A. Tschumi, B. Lee, M. Poidinger,
733 F. Zolezzi, L. Quagliata, P. Sander, E. Newell, A. Bertoletti, L. Terracciano, G. De Libero, L.
734 Mori, Parallel T-cell cloning and deep sequencing of human MAIT cells reveal stable oligoclonal
735 TCRβ 2 repertoire. *Nat. Commun.* **5** (2014), doi:10.1038/ncomms4866.
736 30. E. Martin, E. Treiner, L. Duban, L. Guerri, H. Laude, C. Toly, V. Premel, A. Devys, I. C. Moura,
737 F. Tilloy, S. Cherif, G. Vera, S. Latour, C. Soudais, O. Lantz, Stepwise Development of MAIT
738 Cells in Mouse and Human. *PLoS Biol.* **7**, e1000054 (2009).
739 31. L. Le Bourhis, E. Martin, I. Péguillet, A. Guihot, N. Froux, M. Coré, E. Lévy, M. Dusseaux, V.
740 Meyssonnier, V. Premel, C. Ngo, B. Riteau, L. Duban, D. Robert, M. Rottman, C. Soudais, O.
741 Lantz, Antimicrobial activity of mucosal-associated invariant T cells. *Nat. Immunol.* **11**, 701–708
742 (2010).
743 32. M. Dusseaux, E. Martin, N. Serriari, I. Péguillet, V. Premel, D. Louis, M. Milder, L. Le Bourhis,
744 C. Soudais, E. Treiner, O. Lantz, Human MAIT cells are xenobiotic-resistant, tissue-targeted,
745 CD161 hi IL-17-secreting T cells. *Blood*. **117**, 1250–1259 (2011).

746 33. A. Rahimpour, H. F. Koay, A. Enders, R. Clanchy, S. B. G. Eckle, B. Meehan, Z. Chen, B.
747 Whittle, L. Liu, D. P. Fairlie, C. C. Goodnow, J. McCluskey, J. Rossjohn, A. P. Uldrich, D. G.
748 Pellicci, D. I. Godfrey, Identification of phenotypically and functionally heterogeneous mouse
749 mucosal-associated invariant T cells using MR1 tetramers. *J. Exp. Med.* **212**, 1095–1108 (2015).
750 34. A. Kurioka, J. E. Ussher, C. Cosgrove, C. Clough, J. R. Fergusson, K. Smith, Y. H. Kang, L. J.
751 Walker, T. H. Hansen, C. B. Willberg, P. Klenerman, MAIT cells are licensed through granzyme
752 exchange to kill bacterially sensitized targets. *Mucosal Immunol.* **8**, 429–440 (2015).
753 35. L. Le Bourhis, M. Dusseaux, A. Bohineust, S. Bessoles, E. Martin, V. Premel, M. Coré, D. Sleurs,
754 N. E. Serriari, E. Treiner, C. Hivroz, P. Sansonetti, M. L. Gougeon, C. Soudais, O. Lantz, MAIT
755 Cells Detect and Efficiently Lyse Bacterially-Infected Epithelial Cells. *PLoS Pathog.* **9** (2013),
756 doi:10.1371/journal.ppat.1003681.
757 36. J. Dias, E. Leeansyah, J. K. Sandberg, Multiple layers of heterogeneity and subset diversity in
758 human MAIT cell responses to distinct microorganisms and to innate cytokines. *Proc. Natl. Acad.*
759 *Sci.* **114**, E5434–E5443 (2017).
760 37. A. Meierovics, W.-J. C. Yankelevich, S. C. Cowley, MAIT cells are critical for optimal mucosal
761 immune responses during in vivo pulmonary bacterial infection. *Proc. Natl. Acad. Sci.* **110**,
762 E3119–E3128 (2013).
763 38. P. Georgel, M. Radosavljevic, C. Macquin, S. Bahram, The non-conventional MHC class I MR1
764 molecule controls infection by Klebsiella pneumoniae in mice. *Mol. Immunol.* **48**, 769–775
765 (2011).
766 39. Z. Chen, H. Wang, C. D'Souza, S. Sun, L. Kostenko, S. B. G. Eckle, B. S. Meehan, D. C. Jackson,
767 R. A. Strugnell, H. Cao, N. Wang, D. P. Fairlie, L. Liu, D. I. Godfrey, J. Rossjohn, J. McCluskey,
768 A. J. Corbett, Mucosal-associated invariant T-cell activation and accumulation after in vivo
769 infection depends on microbial riboflavin synthesis and co-stimulatory signals. *Mucosal Immunol.*
770 **10**, 58–68 (2017).

771 40. H. Wang, C. D'Souza, X. Y. Lim, L. Kostenko, T. J. Pediongco, S. B. G. Eckle, B. S. Meehan, M.
772 Shi, N. Wang, S. Li, L. Liu, J. Y. W. Mak, D. P. Fairlie, Y. Iwakura, J. M. Gunnersen, A. W.
773 Stent, D. I. Godfrey, J. Rossjohn, G. P. Westall, L. Kjer-Nielsen, R. A. Strugnell, J. McCluskey,
774 A. J. Corbett, T. S. C. Hinks, Z. Chen, MAIT cells protect against pulmonary Legionella
775 longbeachae infection. *Nat. Commun.* **9**, 3350 (2018).
776 41. F. J. Radcliff, S. Waldvogel-thurlow, F. Clow, M. Mahadevan, J. Johnston, G. Li, T. Proft, R. G.
777 Douglas, J. D. Fraser, Impact of Superantigen-Producing Bacteria on T Cells from Tonsillar
778 Hyperplasia. *Pathogens.* **8**, 1–17 (2019).
779 42. E. Leeansyah, L. Loh, D. F. Nixon, J. K. Sandberg, Acquisition of innate-like microbial reactivity
780 in mucosal tissues during human fetal MAIT-cell development. *Nat. Commun.* **5**, 1–10 (2014).
781 43. P. A. Szabo, M. Miron, D. L. Farber, Location, location, location: Tissue resident memory T cells
782 in mice and humans. *Sci. Immunol.* **4**, 1–12 (2019).
783 44. M. L. Freeman, S. R. Morris, M. M. Lederman, CD161 Expression on Mucosa-Associated
784 Invariant T Cells is Reduced in HIV-Infected Subjects Undergoing Antiretroviral Therapy Who
785 Do Not Recover CD4+ T Cells. *Pathog. Immun.* **2**, 335 (2017).
786 45. A. Han, J. Glanville, L. Hansmann, M. M. Davis, Linking T-cell receptor sequence to functional
787 phenotype at the single-cell level. *Nat. Biotechnol.* **32**, 684–692 (2014).
788 46. V. Voillet, M. Buggert, C. K. Slichter, J. D. Berkson, F. Mair, M. M. Addison, Y. Dori, G.
789 Nadolski, M. G. Itkin, R. Gottardo, M. R. Betts, M. Prlic, Human MAIT cells exit peripheral
790 tissues and recirculate via lymph in steady state conditions. *JCI insight*. **3**, 1–10 (2018).
791 47. L. Loh, N. A. Gherardin, S. Sant, J. C. Crawford, N. L. Bird, C. E. Van De Sandt, M. L. Moreira,
792 E. K. Allen, J. Crowe, T. Loudovaris, K. L. Flanagan, K. M. Quinn, J. Rossjohn, G. Paul, S. B. G.
793 Eckle, J. Mccluskey, I. Dale, K. Kedzierska, J. C. Crawford, N. L. Bird, H. Koay, C. E. Van De
794 Sandt, M. L. Moreira, M. Lappas, E. K. Allen, J. Crowe, T. Loudovaris, K. L. Flanagan, K. M.
795 Quinn, J. Rossjohn, P. G. Thomas, Human Mucosal-Associated Invariant T Cells in Older

796 Individuals Display Expanded TCR α β Clonotypes with Potent Antimicrobial Responses (2020),
797 doi:10.4049/jimmunol.1900774.
798 48. M. C. Gold, J. E. McLaren, J. A. Reistetter, S. Smyk-Pearson, K. Ladell, G. M. Swarbrick, Y. Y.
799 L. Yu, T. H. Hansen, O. Lund, M. Nielsen, B. Gerritsen, C. Kesmir, J. J. Miles, D. A. Lewinsohn,
800 D. A. Price, D. M. Lewinsohn, MR1-restricted MAIT cells display ligand discrimination and
801 pathogen selectivity through distinct T cell receptor usage. *J. Exp. Med.* **211**, 1601–1610 (2014).
802 49. K. Franciszkiewicz, M. Salou, F. Legoux, Q. Zhou, Y. Cui, S. Bessoles, O. Lantz, MHC class I-
803 related molecule, MR1, and mucosal-associated invariant T cells. *Immunol. Rev.* **272**, 120–138
804 (2016).
805 50. M. I. Vazquez, J. Catalan-Dibene, A. Zlotnik, B cells responses and cytokine production are
806 regulated by their immune microenvironment. *Cytokine*. **74**, 318–326 (2015).
807 51. A. G. Zaretsky, J. J. Taylor, I. L. King, F. A. Marshall, M. Mohrs, E. J. Pearce, T follicular helper
808 cells differentiate from Th2 cells in response to helminth antigens. *J. Exp. Med.* **206**, 991–999
809 (2009).
810 52. D. Fang, K. Cui, K. Mao, G. Hu, R. Li, M. Zheng, N. Riteau, S. L. Reiner, A. Sher, K. Zhao, J.
811 Zhu, Transient T-bet expression functionally specifies a distinct T follicular helper subset. *J. Exp.*
812 *Med.* **215**, 2705–2714 (2018).
813 53. P. Wang, Y. Wang, L. Xie, M. Xiao, J. Wu, L. Xu, Q. Bai, Y. Hao, Q. Huang, X. Chen, R. He, B.
814 Li, S. Yang, Y. Chen, Y. Wu, L. Ye, The transcription factor T-bet is required for optimal type I
815 follicular helper T cell maintenance during acute viral infection. *Front. Immunol.* **10**, 1–17 (2019).
816 54. K. Li, C. K. Vorkas, A. Chaudhry, D. L. Bell, R. A. Willis, A. Rudensky, J. D. Altman, M. S.
817 Glickman, J. Aubé, Synthesis, stabilization, and characterization of the MR1 ligand precursor 5-
818 amino-6-D-ribitylaminouracil (5-A-RU). *PLoS One*. **13**, 20–22 (2018).
819 55. J. Shen, X. Luo, Q. Wu, J. Huang, G. Xiao, L. Wang, B. Yang, H. Li, C. Wu, A subset of
820 CXCR5+CD8+ T cells in the germinal centers from human tonsils and lymph nodes help B cells

821 produce immunoglobulins. *Front. Immunol.* **9**, 1–12 (2018).
822 56. T. Leng, H. D. Akther, C. P. Hackstein, K. Powell, T. King, M. Friedrich, Z. Christoforidou, S.
823 McCuaig, M. Neyazi, C. V. Arancibia-Cárcamo, J. Hagel, F. Powrie, R. S. Peres, V. Millar, D.
824 Ebner, R. Lamichhane, J. Ussher, T. S. C. Hinks, E. Marchi, C. Willberg, P. Klenerman, TCR and
825 Inflammatory Signals Tune Human MAIT Cells to Exert Specific Tissue Repair and Effector
826 Functions. *Cell Rep.* **28**, 3077-3091.e5 (2019).
827 57. M. Lettau, A. Wiedemann, E. V. Schrezenmeier, C. Giesecke-Thiel, T. Dörner, Human CD27+
828 memory B cells colonize a superficial follicular zone in the palatine tonsils with similarities to the
829 spleen. A multicolor immunofluorescence study of lymphoid tissue. *PLoS One*. **15**, 1–17 (2020).
830 58. E. Donnadieu, K. B. Reisinger, S. Scharf, Y. Michel, J. Bein, S. Hansen, A. G. Loth, N. Flinner, S.
831 Hartmann, M.-L. Hansmann, Landscape of T Follicular Helper Cell Dynamics in Human
832 Germinal Centers. *J. Immunol.*, ji1901475 (2020).
833 59. J. J. Hong, P. K. Amancha, K. Rogers, A. A. Ansari, F. Villinger, Spatial Alterations between
834 CD4 + T Follicular Helper, B, and CD8 + T Cells during Simian Immunodeficiency Virus
835 Infection: T/B Cell Homeostasis, Activation, and Potential Mechanism for Viral Escape . *J.*
836 *Immunol.* **188**, 3247–3256 (2012).
837 60. J. A. Kotov, M. K. Jenkins, Cutting Edge: T Cell–Dependent Plasmablasts Form in the Absence of
838 Single Differentiated CD4 $^{+}$ T Cell Subsets. *J. Immunol.*, ji1801349 (2018).
839 61. E. Nygren, J. Holmgren, S. R. Attridge, Murine antibody responses following systemic or mucosal
840 immunization with viable or inactivated Vibrio cholerae. *Vaccine*. **26**, 6784–6790 (2008).
841 62. I. S. Cisternas, A. Torres, A. F. Flores, V. A. G. Angulo, Differential regulation of riboflavin
842 supply genes in Vibrio cholerae. *Gut Pathog.* **9**, 1–7 (2017).
843 63. D. J. Haney, M. D. Lock, J. K. Simon, J. Harris, M. Gurwith, Antibody-based correlates of
844 protection against cholera: Analysis of a challenge study of a cholera-naive population. *Clin.*
845 *Vaccine Immunol.* **24**, 1–11 (2017).

846 64. J. B. Harris, R. C. LaRocque, F. Chowdhury, A. I. Khan, T. Logvinenko, A. S. G. Faruque, E. T.
847 Ryan, F. Qadri, S. B. Calderwood, Susceptibility to Vibrio cholerae infection in a cohort of
848 household contacts of patients with cholera in Bangladesh. *PLoS Negl. Trop. Dis.* **2** (2008),
849 doi:10.1371/journal.pntd.0000221.
850 65. R. Finkelstein, Vibriocidal Antibody Inhibition (VAI) Analysis: A Technique for the Identification
851 of the Predominant Vibriocidal Antibodies in Serum and for the Detection and Identification of
852 Vibrio Cholerae Antigens. *J. Immunol.* **89**, 264–271 (1962).
853 66. R. I. Glass, A. M. Svennerholm, M. R. Khan, S. Huda, M. Imdadul Huq, J. Holmgren,
854 Seroepidemiological studies of EI tor cholera in bangladesh: Association of serum antibody levels
855 with protection. *J. Infect. Dis.* **151**, 236–242 (1985).
856 67. A. S. Azman, J. Lessler, F. J. Luquero, T. R. Bhuiyan, A. I. Khan, F. Chowdhury, A. Kabir, M.
857 Gurwith, A. A. Weil, J. B. Harris, S. B. Calderwood, E. T. Ryan, F. Qadri, D. T. Leung,
858 Estimating cholera incidence with cross-sectional serology. *Sci. Transl. Med.* **11**, 1–11 (2019).
859 68. D. T. Leung, T. Uddin, P. Xu, A. Aktar, R. A. Johnson, M. A. Rahman, M. M. Alam, M. K.
860 Bufano, G. Eckhoff, Y. Wu-Freeman, Y. Yu, T. Sultana, F. Khanam, A. Saha, F. Chowdhury, A. I.
861 Khan, R. C. Charles, R. C. LaRocque, J. B. Harris, S. B. Calderwood, P. Kováč, F. Qadri, E. T.
862 Ryan, Immune responses to the O-specific polysaccharide antigen in children who received a
863 killed oral cholera vaccine compared to responses following natural cholera infection in
864 Bangladesh. *Clin. Vaccine Immunol.* **20**, 780–788 (2013).
865 69. S. M. Patel, M. A. Rahman, M. Mohasin, M. A. Riyadh, D. T. Leung, M. M. Alam, F.
866 Chowdhury, A. I. Khan, A. A. Weil, A. Aktar, M. Nazim, R. C. LaRocque, E. T. Ryan, S. B.
867 Calderwood, F. Qadri, J. B. Harris, Memory B Cell Responses to Vibrio cholerae O1
868 Lipopolysaccharide Are Associated with Protection against Infection from Household Contacts of
869 Patients with Cholera in Bangladesh. *Clin. Vaccine Immunol.* **19**, 842–848 (2012).
870 70. A. S. Iyer, A. S. Azman, M. Bouhenia, L. O. Deng, C. P. Anderson, M. Graves, P. Kováč, P. Xu,

871 E. T. Ryan, J. B. Harris, D. A. Sack, F. J. Luquero, D. T. Leung, Dried Blood Spots for Measuring
872 Vibrio cholerae-specific Immune Responses. *PLoS Negl. Trop. Dis.* **12** (2018),
873 doi:10.1371/journal.pntd.0006196.
874 71. R. C. Kauffman, T. R. Bhuiyan, R. Nakajima, L. M. Mayo-Smith, R. Rashu, M. R. Hoq, F.
875 Chowdhury, A. I. Khan, A. Rahman, S. K. Bhaumik, L. Harris, J. T. O'Neal, J. F. Trost, N. H.
876 Alam, A. Jasinskas, E. Dotsey, M. Kelly, R. C. Charles, P. Xu, P. Kováč, S. B. Calderwood, E. T.
877 Ryan, P. L. Felgner, F. Qadri, J. Wrammert, J. B. Harris, Single-cell analysis of the plasmablast
878 response to Vibrio cholerae demonstrates expansion of cross-reactive memory B cells. *MBio*. **7**, 1–
879 11 (2016).
880 72. B. Sit, T. Zhang, B. Fakoya, A. Akter, R. Biswas, E. T. Ryan, M. K. Waldor, Oral immunization
881 with a probiotic cholera vaccine induces broad protective immunity against Vibrio cholerae
882 colonization and disease in mice. *PLoS Negl. Trop. Dis.*, 1–20 (2019).
883 73. N. Rout, Enhanced Th1/Th17 Functions of CD161+ CD8+ T Cells in Mucosal Tissues of Rhesus
884 Macaques. *PLoS One*. **11**, e0157407 (2016).
885 74. S. Crotty, T Follicular Helper Cell Differentiation, Function, and Roles in Disease. *Immunity*. **41**,
886 529–542 (2014).
887 75. M. Salio, O. Gasser, C. Gonzalez-Lopez, A. Martens, N. Veerapen, U. Gileadi, J. G. Verter, G.
888 Napolitani, R. Anderson, G. Painter, G. S. Besra, I. F. Hermans, V. Cerundolo, Activation of
889 Human Mucosal-Associated Invariant T Cells Induces CD40L-Dependent Maturation of
890 Monocyte-Derived and Primary Dendritic Cells. *J. Immunol.*, ji1700615 (2017).
891 76. R. J. Johnston, A. C. Poholek, D. DiToro, I. Yusuf, D. Eto, B. Barnett, A. L. Dent, J. Craft, S.
892 Crotty, Bcl6 and Blimp-1 are reciprocal and antagonistic regulators of T follicular helper cell
893 differentiation. *Science (80-.).* **325**, 1006–1010 (2009).
894 77. R. Ettinger, S. Kuchen, P. E. Lipsky, The role of IL-21 in regulating B-cell function in health and
895 disease. *Immunol. Rev.* **223**, 60–86 (2008).

896 78. D. Eto, C. Lao, D. DiToro, B. Barnett, T. C. Escobar, R. Kageyama, I. Yusuf, S. Crotty, IL-21 and
897 IL-6 are critical for different aspects of B cell immunity and redundantly induce optimal follicular
898 helper CD4 T cell (Tfh) differentiation. *PLoS One*. **6**, e17739 (2011).
899 79. L. Moens, S. G. Tangye, Cytokine-mediated regulation of plasma cell generation: IL-21 takes
900 center stage. *Front. Immunol.* **5**, 1–13 (2014).
901 80. A. Cerutti, M. Cols, I. Puga, Activation of B cells by non-canonical helper signals. *EMBO Rep.* **13**,
902 798–810 (2012).
903 81. X. Shen, T. Lagergard, Y. Yang, M. Lindblad, M. Fredriksson, J. Holmgren, Systemic and
904 mucosal immune responses in mice after mucosal immunization with group B streptococcus type
905 III capsular polysaccharide-cholera toxin B subunit conjugate vaccine. *Infect. Immun.* **68**, 5749–
906 5755 (2000).
907 82. H. Yu, A. Yang, S. Derrick, J. Y. W. Mak, L. Liu, D. P. Fairlie, S. Cowley, Artificially induced
908 MAIT cells inhibit M . bovis BCG but not M . tuberculosis during in vivo pulmonary infection.
909 *Sci. Rep.*, 1–12 (2020).
910 83. S. Sakai, K. D. Kauffman, S. Oh, C. E. Nelson, C. E. B. Iii, D. L. Barber, MAIT cell-directed
911 therapy of Mycobacterium tuberculosis infection. *Mucosal Immunol.*, 1–10 (2020).
912 84. A. Cerutti, The regulation of IgA class switching. *Nat. Rev. Immunol.* **8**, 421–434 (2008).
913 85. J. Holmgren, A. M. Svennerholm, Vaccines against mucosal infections. *Curr. Opin. Immunol.* **24**,
914 343–353 (2012).
915 86. G. Ben Youssef, M. Tourret, M. Salou, L. Ghazarian, V. Houdouin, S. Mondot, Y. Mburu, M.
916 Lambert, S. Azarnoush, J.-S. Diana, A.-L. Virlouvet, M. Peuchmaur, T. Schmitz, J.-H. Dalle, O.
917 Lantz, V. Biran, S. Caillat-Zucman, Ontogeny of human mucosal-associated invariant T cells and
918 related T cell subsets. *J. Exp. Med.* **215**, 459–479 (2018).
919 87. F. Legoux, M. Salou, O. Lantz, MAIT Cell Development and Functions: the Microbial
920 Connection. *Immunity*. **53**, 710–723 (2020).

921 88. F. Qadri, G. Mohi, J. Hossain, T. Azim, A. M. Khan, M. A. Salam, R. B. Sack, M. J. Albert, A. M.
922 Svennerholm, Comparison of the vibriocidal antibody response in cholera due to Vibrio cholerae
923 O139 Bengal with the response in cholera due to Vibrio cholerae O1. *Clin. Diagn. Lab. Immunol.*
924 **2**, 685–8 (1995).
925 89. P. Mombaerts, A. R. Clarke, M. A. Rudnicki, J. Iacomini, S. Itohara, J. J. Lafaille, L. Wang, Y.
926 Ichikawa, R. Jaenisch, M. L. Hooper, S. Tonegawa, Mutations in T-cell antigen receptor genes α
927 and β block thymocyte development at different stages. *Nature*. **360**, 225–231 (1992).
928
929
930

931 **Acknowledgements**

932 **Funding:** This research was supported by the National Institutes of Health (R01 AI130378 to D.T.L. and
933 T32 AI138945 to O.J.). This work was also supported by the University of Utah Flow Cytometry Facility
934 in addition to the National Cancer Institute through Award Number P30CA042014. We would also like to
935 thank the staff of the Office of Comparative Medicine, and University of Utah Cell Imaging Core, and
936 Kelin Li and Jeffrey Aubé (UNC Chapel Hill) for providing 5-amino-6-D-ribitylaminouracil (5-A-RU)
937 for our study.

938 **Author Contributions:** O.J. and D.T.L. designed and directed the project. O.J and S.T. performed the
939 experiments. K.F. and J.S.H. contributed to experimental methodology. J.D.M. provided samples and
940 resources. D.T.L acquired funding. O.J. and D.T.L wrote the paper, and all authors discussed results,
941 provided critical feedback, and contributed to the final manuscript.

942 **Declaration of interests:** None.

943

944 **Supplementary Materials**

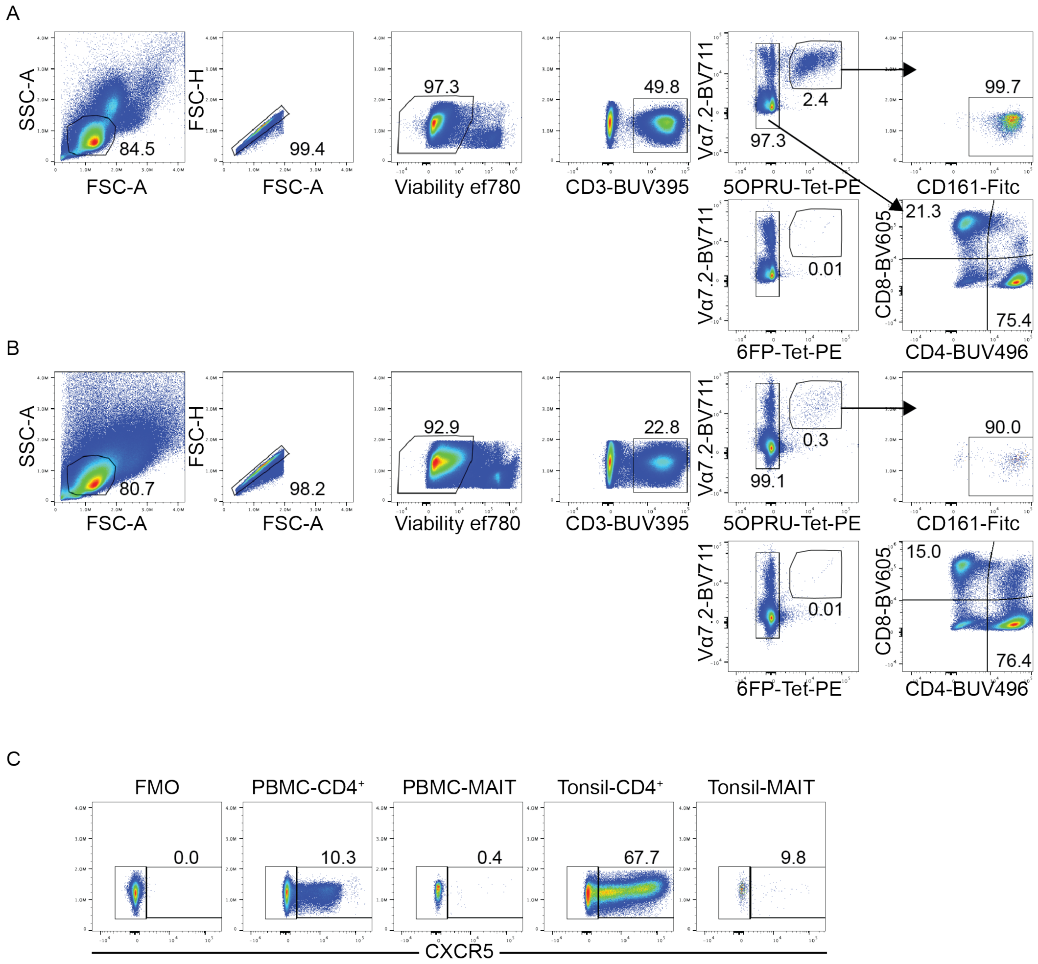

945

Supplementary Fig. 1. Representative flow cytometry gating strategy for Fig. 1. Representative flow cytometry gating strategy for MAIT and non-MAIT T cells in (**A**) PBMC and (**B**) tonsils. PE conjugated 6-FP MR1-Tetramer gating controls for PBMC and tonsils are located below 5-OP-RU MR1-Tetramer staining gates. (**C**) Representative CXCR5 staining for PBMC and tonsil $CD4^+$ T and MAIT cells quantified in Fig. 1C. Gating was based on CXCR5 fluorescence minus one (FMO) control.

946
947

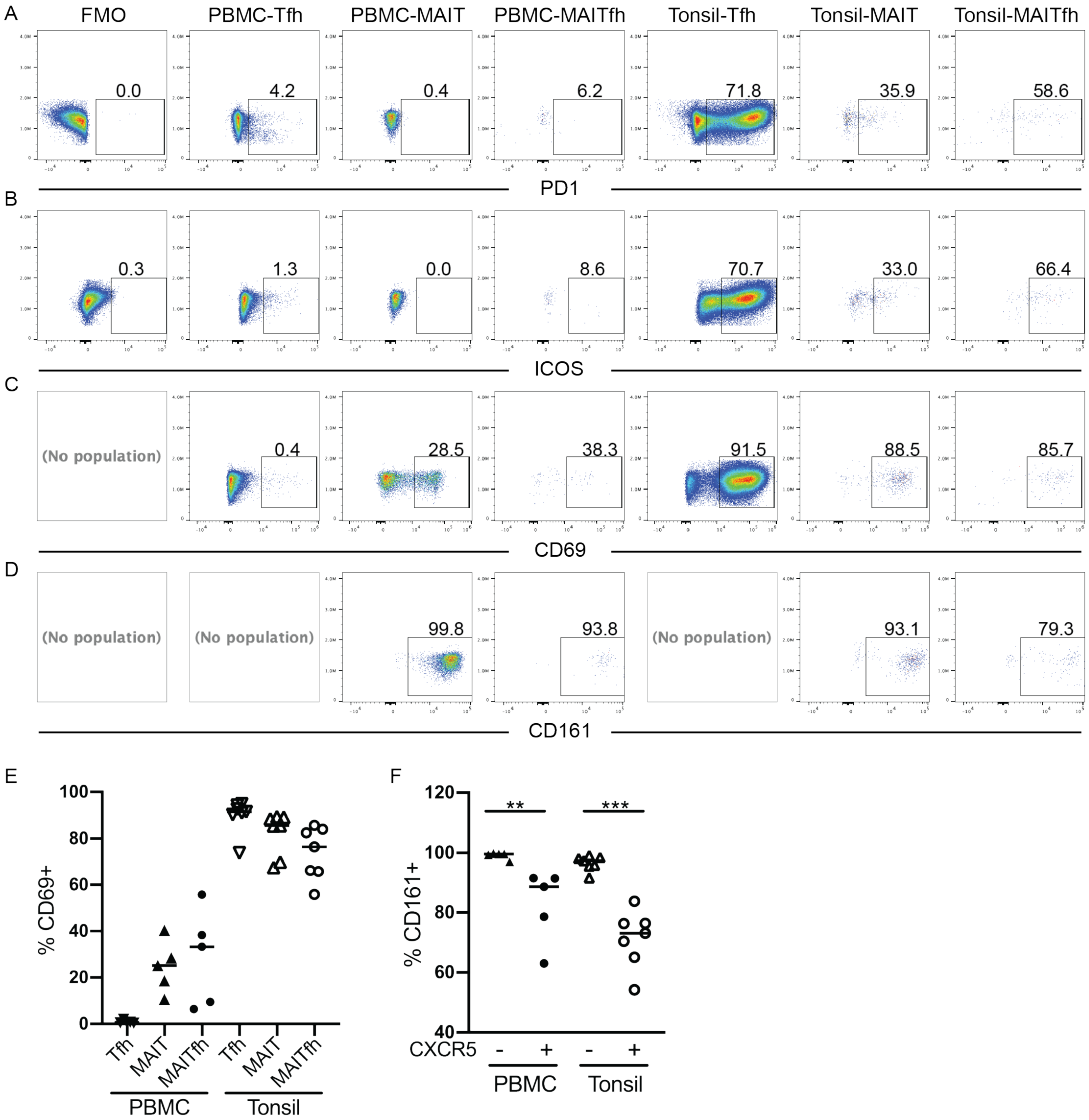

Supplementary Fig. 2. Flow gating strategy for T cell co-stimulatory molecule expression analysis. Representative flow cytometry gating strategy for PBMC and tonsil Tfh, MAIT and MAITfh cell (**A**) PD1, (**B**) ICOS, (**C**) CD69, and (**D**) CD161 expression. FMO's were not included for CD69 and CD161 due to clarity of antibody staining. (**E**) Frequency of Tfh, MAIT, and MAITfh cell populations expressing CD69. (**F**) Frequency of $CD161^{+}$ MAIT cells broken down by CXCR5 expression. Data are represented as median from 1 independent experiment. n = 5-7. *p < 0.05, **p<0.01, ***p<0.001, ****p<0.0001 by two-tailed Mann-Whitney U test.

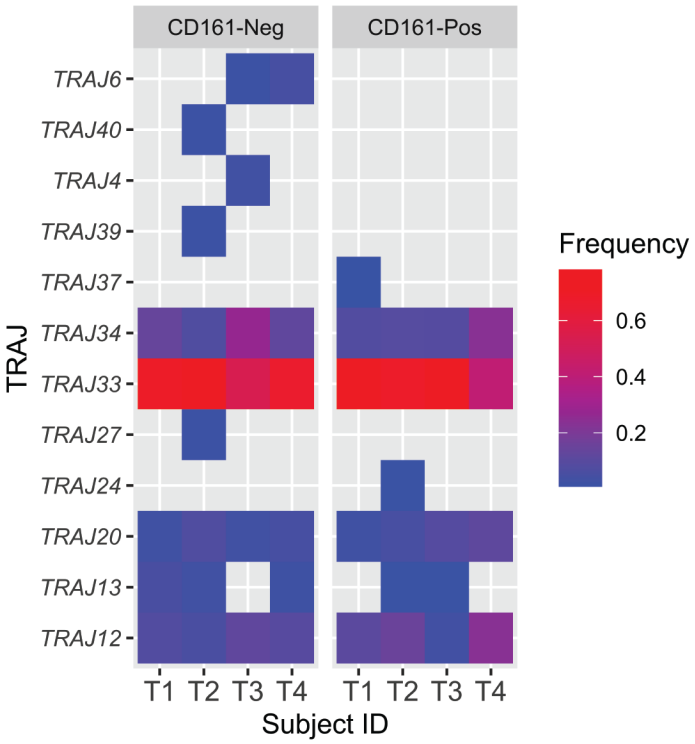

952
953

Supplementary Fig. 3. Similar TRAJ expression in CD161+ and CD161- tonsil MAIT cells. Heat map of TRAJ usage percent frequencies based on Illumina single cell TCR-Phenotype sequencing in tonsil MAIT cells broken down by CD161 negative (top) and positive (bottom) populations. Each column represents an individual donor (n=4). MAIT cells were defined as MR1-5-OP-RU-tetramer positive, and TRAV1-2 antibody positive. No statistical significance was found between CD161- and CD161+ groups using Multiple t tests comparison accounting for False Discoveries using the Benjamini, Krieger and Yekutieli method.

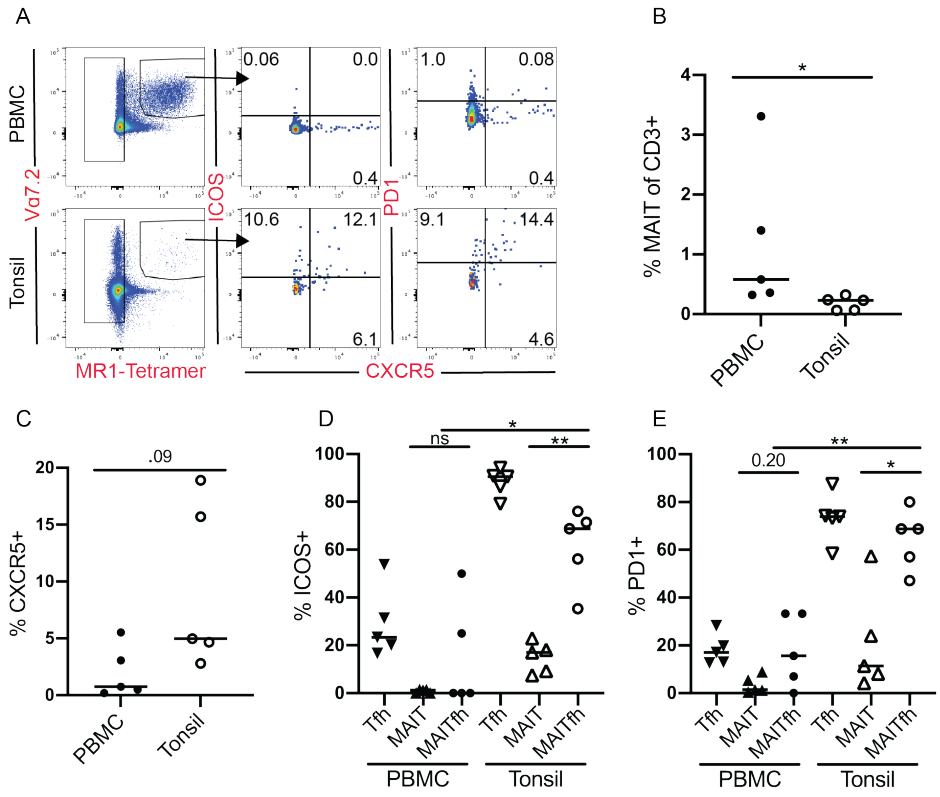

Supplementary Fig. 4. Tfh co-stimulatory marker expression in paired pediatric tonsil and PBMC samples. (**A**) Representative FACS plots of unstimulated paired pediatric $CD3^+$ PBMC (top) and tonsil (bottom) donor cells with MAIT cell (gated in left panel) co-expression of CXCR5 with ICOS (middle) and PD1 (right). (**B**) Quantification of MAIT cell frequency as percentage of $CD3^+$. (**C**) Frequency of $CXCR5^+$ MAIT cells. Frequency of (**D**) $ICOS^+$ and (**E**) $PD1^+$ MAIT, MAITfh and Tfh cells. Data are represented as Median from 2 pooled independent experiments. n ≥ 13. *$p < 0.05$, **$p<0.01$, ***$p<0.001$, ****$p<0.0001$ by two-tailed Mann-Whitney *U* test

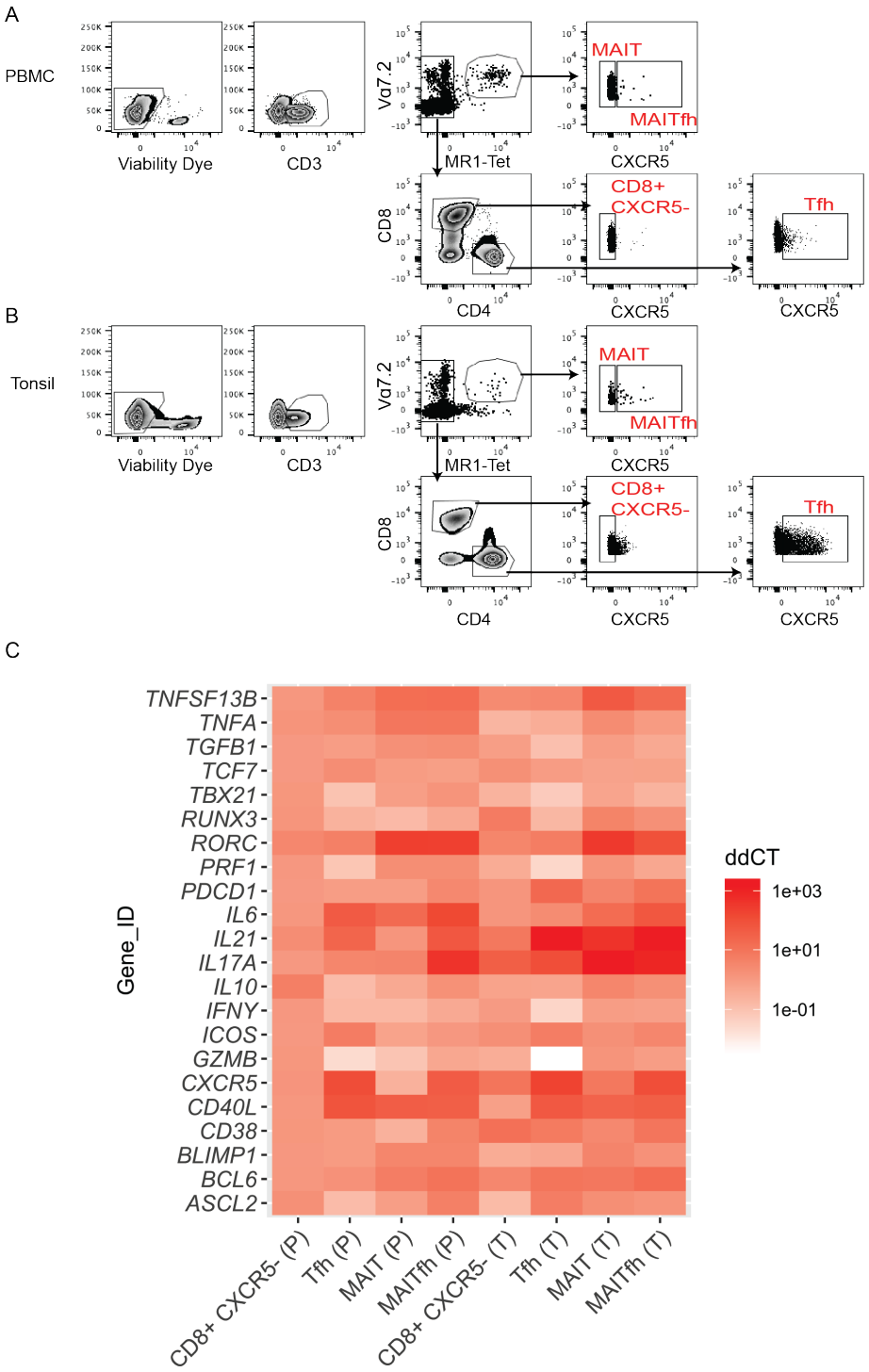

Supplementary Fig. 5. qPCR and flow gating strategy (Fig 2) and additional FAC sorted qPCR targets. Representative flow cytometry gating strategy for qPCR FAC sorted and flow populations in Fig.2 from (**A**) PBMC and (**B**) tonsils. (**C**) Heat map of additional qPCR targets described in Fig 2. As described, data are represented as ΔΔCt relative to β-Actin and then the PBMC-CD8^{+}CXCR5^{-} population. Rows denote gene ID and columns denote sample group (P=PBMC, T=tonsil). Heat map data are represented by mean of n=6-8 samples per group.

958

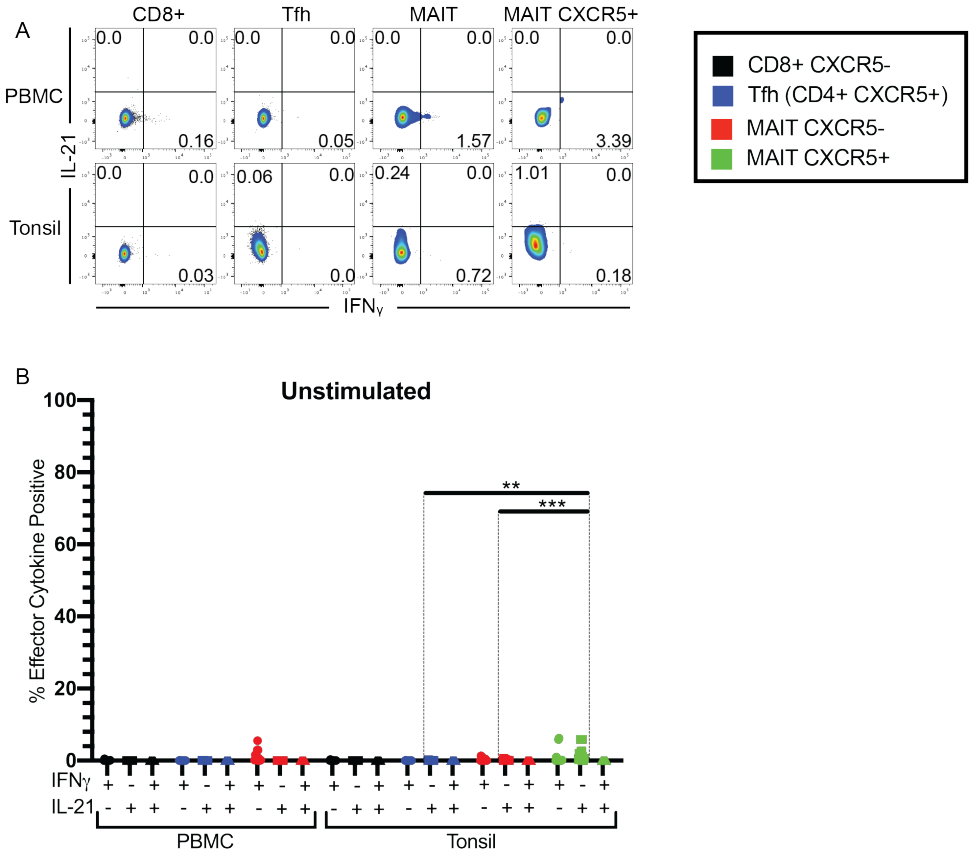

959

Supplementary Fig. 6. IFNγ and IL-21 expression in unstimulated PMBC and tonsil T cell populations. (**A**) Representative flow cytometry from 6 hour no stimulation controls with BFA added for final 4 hours in PBMC and tonsil T cell populations showing IL-21 and IFNγ co-expression. (**B**) Frequency of T cell populations expressing IL-21, IFNγ or both. Data are represented as median from two pooled independent experiments. n≥5. *$p < 0.05$, **$p<0.01$, ***$p<0.001$, ****$p<0.0001$ by two-tailed Mann-Whitney *U* test. Legend in black box denotes experimental groups.

960
961
962
963
964

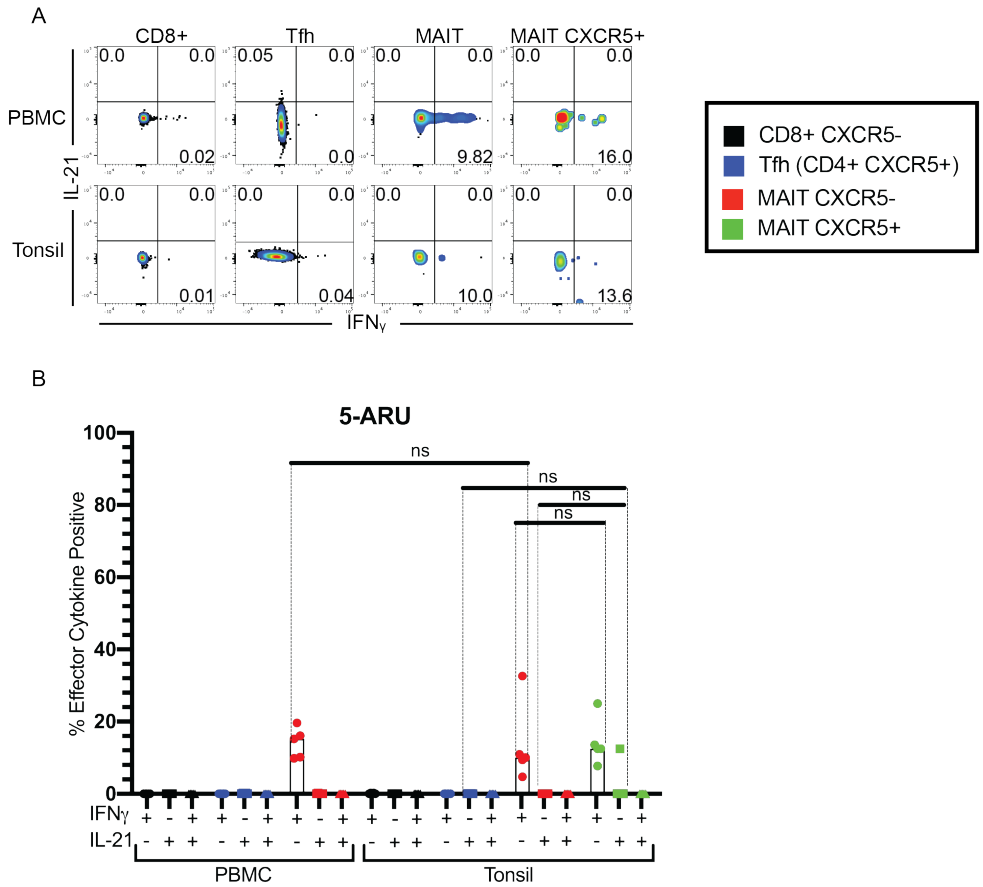

Supplementary Fig. 7. IFNγ and IL-21 expression in 5-A-RU stimulated PMBC and tonsil T cell populations. (**A**) Representative flow cytometry of 6 hr 5-A-RU (0.5 μM/ml) and Methylglyoxal (50 μg/ml) stimulated cultures with BFA in PBMC and tonsil T cell populations showing IL-21 and IFNγ co-expression. (**B**) Frequency of T cell populations expressing IL-21, IFNγ or both. Data are represented as median from one independent experiment. n=5. *$p < 0.05$, **$p<0.01$, ***$p<0.001$, ****$p<0.0001$ by two-tailed Mann-Whitney *U* test. Legend in black box denotes experimental groups.

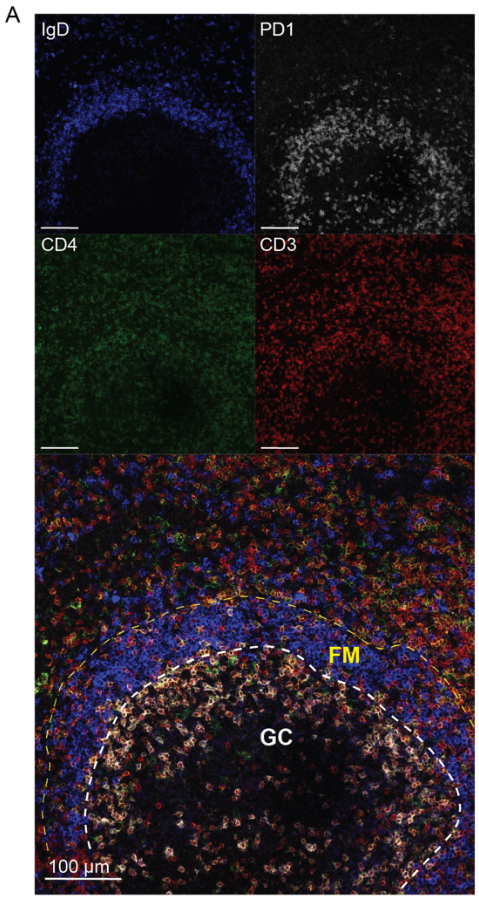

969
970

Supplementary Fig. 8. GC Tfh cells are marked by high PD1 expression in tonsils. (**A**) Representative immunofluorescence images from tonsil cryosections stained with anti-IgD (blue), anti-PD1 (white), anti-CD4 (green), and anti-CD3 (red) and imaged on a Leica SP8 confocal microscope with 20X objective. Enlarged composite image on bottom with a germinal center (GC) highlighted by $PD1^{High}$ GC Tfh cells outlined with white dashed line, and the follicular mantle (FM) made up of IgD^{+} naïve B cells outlined with a yellow dashed line. All scale bars represent 100 µm.

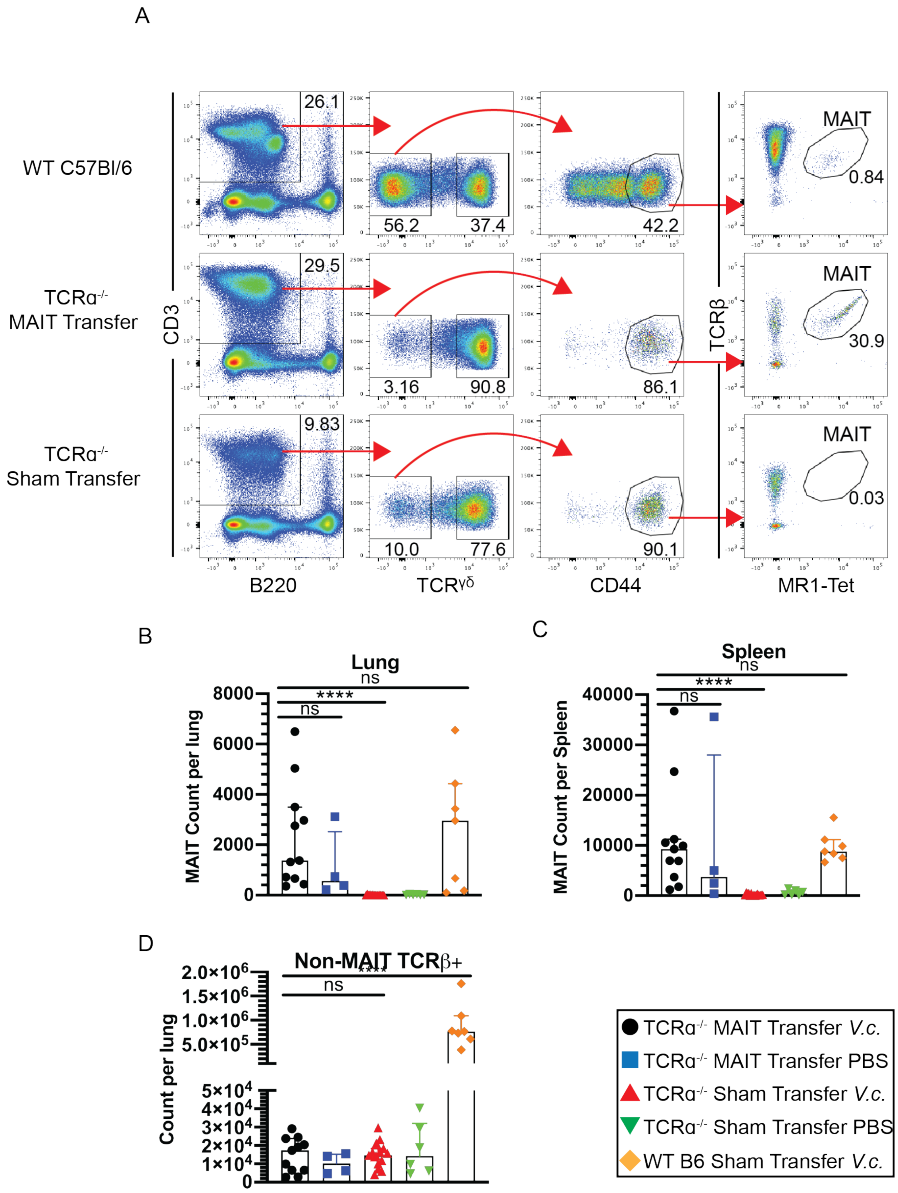

Supplementary Fig. 9. Flow gating for murine lung MAIT and T lymphocyte counts. (**A**) Representative flow gating of murine MAIT cells from digested lung tissue highlighted in Fig. 4a. MAIT cells were defined as live B220^{-} CD3^{+} TCRγδ^{-} CD44^{High} TCRβ^{+} MR1-Tetramer^{+}. Only WT-*V.c.*, MAIT-*V.c.*, and Sham-*V.c.* groups are portrayed. (**B**) Total MAIT cell count per lung. (**C**) Total MAIT cell count per spleen. (D) Total non-MAIT CD3^{+} TCRβ^{+} T cells per lung. Data are represented as Median with IQR from 4 independent experiments. n= 4-15 mice per group. *$p < 0.05$, **$p<0.01$, ***$p<0.001$, ****$p<0.0001$ by two-tailed Mann-Whitney *U* test. Legend in black box denotes experimental groups.

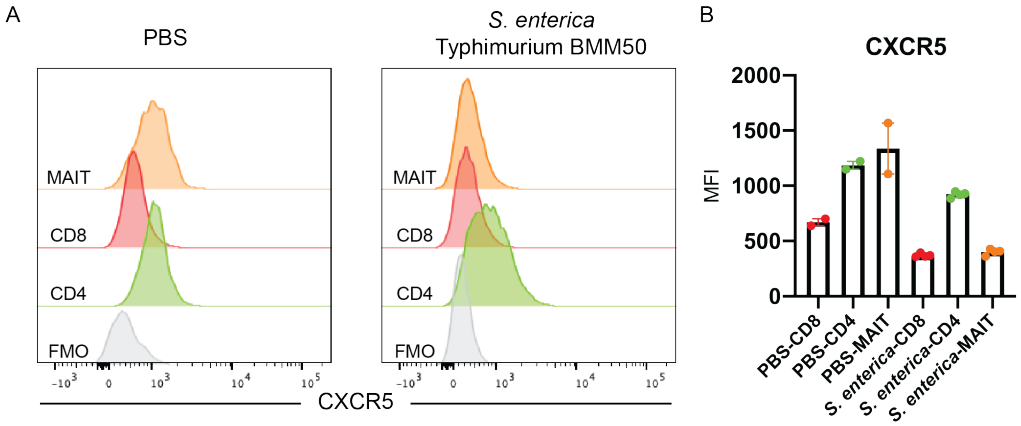

Supplementary Fig. 10. CXCR5 expression on *S. enterica* Typhimurium expanded MAIT cells prior to adoptive transfer. Representative flow cytometry histograms (**A**) and mean fluorescence intensity (**B**) of CXCR5 expression in T cell subsets of Day 7 WT C57Bl/6 mice given intranasal PBS (Left) or 10^6 CFU *S.* Typhimurium (Left). Data are represented as Median from 1 experiment. n= 2-4 mice per group.

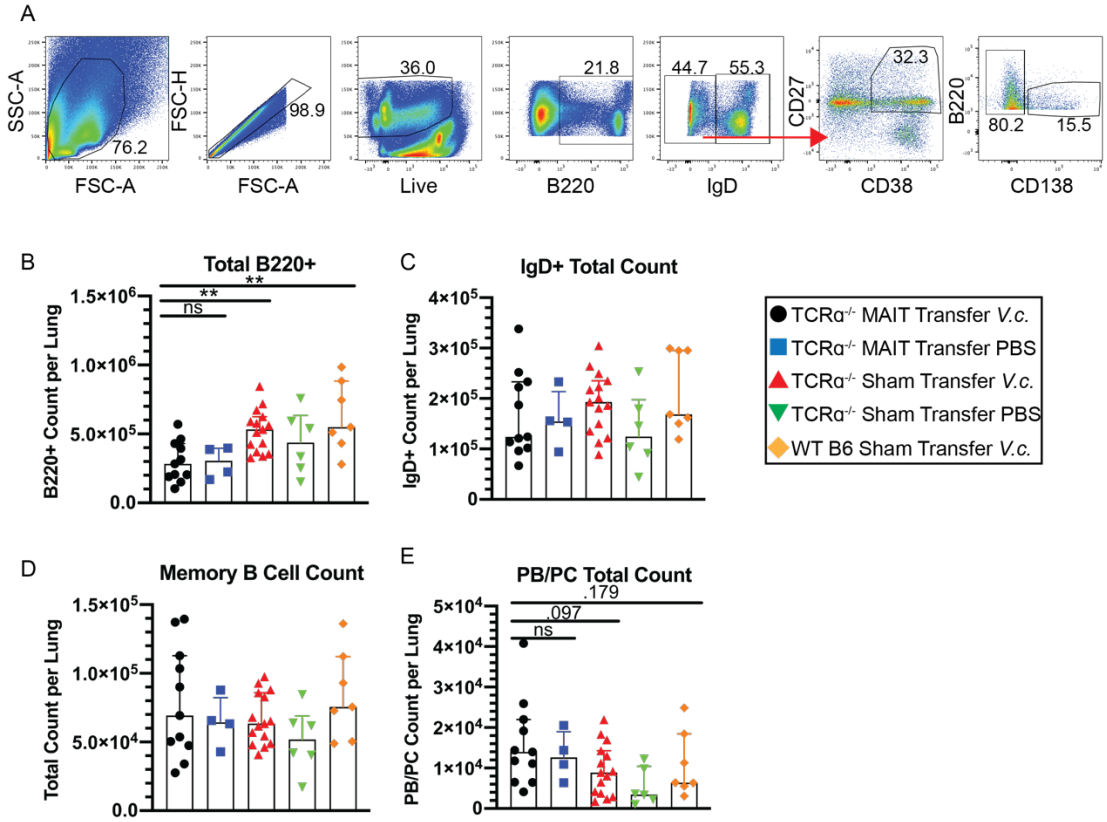

992

Supplementary Fig. 11. Flow gating for murine lung B lymphocyte counts. (**A**) Representative flow cytometry gating strategy of murine B cell subsets from digested lung tissue. (**B**) Total B220^{+} B cells per lung. (**C**) Total B220^{+} IgD^{+} Naïve B cells per lung. (**D**) Total B220^{+} IgD^{-} CD38^{+}CD27^{+}CD138^{-} Memory B cells per lung. (**E**) Total B220^{low} IgD^{-} CD38^{+}CD27^{+}CD138^{+} PB/PCs per lung. Data are represented as Median with IQR from 4 independent experiments. n= 4-15 mice per group. *$p < 0.05$, **$p<0.01$, ***$p<0.001$, ****$p<0.0001$ by two-tailed Mann-Whitney U test. Legend in black box denotes experimental groups.

993
994
995
996
997
998
999

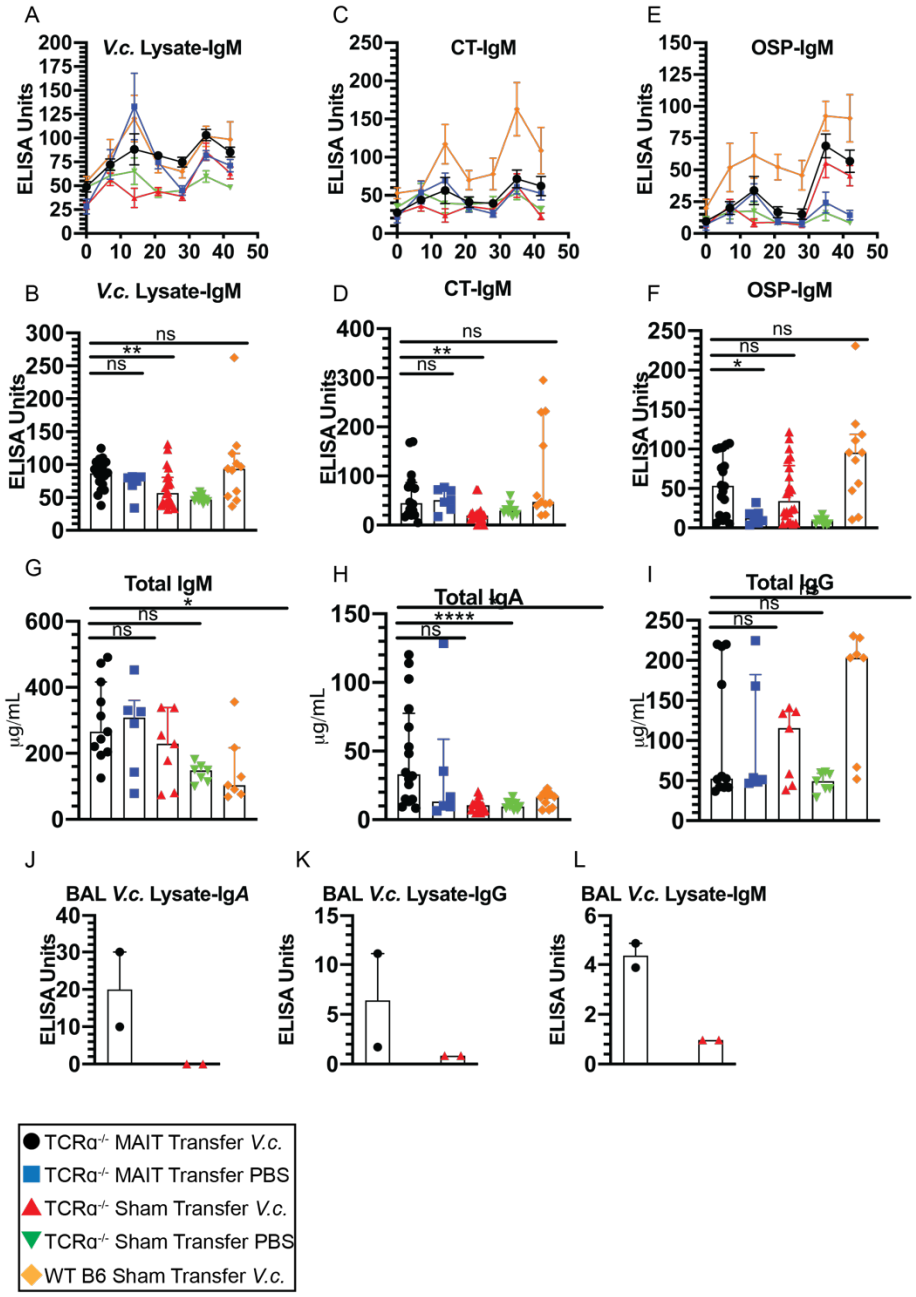

Supplementary Fig. 12. Serum IgM, total IgM, IgG and IgA and BAL fluid ELISAs. (A-F) Serum *V. cholerae* lysate, OSP, and CT IgM ELISAs representing weekly antibody kinetics (A, C & E) and Day 42 endpoint responses (B, D & F). Data are represented as ELISA units normalized to a pooled serum positive control from WT B6 mice challenged with V. cholerae. Total IgM (G), IgA (H) and IgG (I) ELISAs from Day 42 endpoint serum. Total Ig was quantitated using a standard curve based on known Ig quantities. Data are represented as Median with IQR from 5 independent experiments. n= 6-22 mice per group. *p < 0.05, **p<0.01, ***p<0.001, ****p<0.0001 by two-tailed Mann-Whitney U test. *V. cholerae* lysate IgA (J), IgG (K) and IgM (L) ELISAs from D42 BAL fluid. Legend in black box denotes experimental groups.

1000